QUADRUPEDAL EMOTIVE GAITS IN ROBOTICS

by

Travis Brad Hainsworth

A thesis submitted to the faculty of
The University of Utah
in partial fulfillment of the requirements for the degree of

Master of Science

Department of Mechanical Engineering

The University of Utah

August 2017

The University of Utah Graduate School

STATEMENT OF THESIS APPROVAL

The thesis of **Travis Brad Hainsworth**

has been approved by the following supervisory committee members:

Mark Minor	, Chair	**6/13/17** Date Approved
John Hollerbach	, Member	**6/8/17** Date Approved
Andrew Merryweather	, Member	**6/8/17** Date Approved

and by **Tim Ameel** , Chair/Dean of

the Department/College/School of **Mechanical Engineering**

and by David B. Kieda, Dean of The Graduate School.

ABSTRACT

Advances in the field of robotics have laid a solid foundation for human-robot-interaction research; this research values demonstrations of emotional competence from robotic systems and herein lie opportunities for progress within the therapeutic industry, creation of companion robots, and integration of robotics among everyday households. The development of emotive expression within robotics is progressing at a fair pace; however, there is next to no research on this form of expression as it pertains to a robot's manner of walking. The work presented here proves that it is possible for robots to walk with the capability of expressing emotions that are identifiable by their human counterparts.

This hypothesis is explored utilizing a four-legged robot in simulation and reality, and the details necessary for this application are presented in this work. This quadruped is comprised of four manipulators each consisting of seven degrees of freedom. The inverse kinematics and dynamics are solved for each leg with closed form solutions that incorporate the inverse of Euler's finite rotation formula. With the kinematics solved, the robot utilizes a central pattern generator to create a neutral gait and balances with an augmented center of pressure that closely resembles the zero moment point

algorithm. Independent of the kinematics, a method of generating poses that represent the emotions: happy, sad, angry, and fearful, is presented. This work also details how to overlay poses atop a gait to transform the neutral gait into an emotive walking style.

In addition to laying the framework for developing the emotive walking styles, an evaluation of the presented gaits is detailed. Two IRB approved studies were performed independently of each other. The first study took feedback from subjects regarding ways to make the emotive gaits more compelling and applied them to the initial poses. The second study evaluated the effectiveness of the final gaits, with improved poses, and proves that emotive walking patterns were created: walking patterns that will be suitable for emotional acuity.

TABLE OF CONTENTS

LIST OF FIGURES

Figures

LIST OF TABLES

Tables

ACKNOWLEDGMENTS

Special thanks are extended to Kairos Autonomi for providing the hardware used in this study, and thanks are also extended to Dr. Mark A. Minor for his patient tutelage. Thanks are also extended to Dr. John M. Hollerbach for his advice regarding inverse kinematics, and to Dr. Andrew S. Merryweather for his assistance and teaching regarding statistical analysis.

1. INTRODUCTION

Motivation and Approach

To create a robotic system that can empathize with humans is a non-trivial undertaking, requiring extensive use of completed research and a wealth of research yet to be completed. The creation of such a system is necessary to further the field of therapeutic robotics and to make these robotic systems commonplace in the home. For instance, currently, service dogs are used as companions for people diagnosed with autism; however, there are cases where a human with such a handicap may not be capable of physically sustaining a companion animal. In these cases, if a robot was capable of fulfilling the role of a companion, it could sustain itself and fill an emotional void in the patient's life as an in-home companion. Even now, autistic therapy utilizes robotic systems [1], showing that these systems are useful. Yet there is much development to be done in the field.

One facet of this empathetic system that has yet to be formalized is the ability for the system to display an intended emotion using body language. The most related work to this goal has been done using a toy dog and manipulating its walking speed as well as the movement of its head and tail to create simulated emotions [2]. However, this relied heavily on the head

and tail of the robot, and it seems possible for a robotic system to display Ekman's four continuous emotions (happy, sad, anger, and fear) [3, 4] solely through its mode of walking. This development of gaits that can be interpreted as emotional has yet to be shown; that is the goal of this work.

This thesis approaches the challenge of creating a quadrupedal robot, a dog named Mr. Pete, to display emotions through its gaits. We first explore design of the robot legs in order to provide sufficient range of motion to allow redundant poses and foot positions sufficient for displaying different body language. Inverse kinematics are then solved to evaluate how redundancy in the legs can be used to provide different configurations related to different types of body language. The inverse kinematics are then analyzed and modified to assure that particular types of body language are consistently portrayed throughout a gait. A central pattern generator is then used to create quasi-static crawling gaits to create locomotion. Several poses are then created to elicit different emotions, which can be seen in Figure 1. These are then overlaid on top of a neutral pose in combination with the central pattern generator to portray these emotions throughout the gaits while maintain quasi-statically stable postures. IRB-approved external subject studies are then conducted to tune and adapt the poses and gaits to better elicit the perceived emotions. Internal subject studies using a separate subject pool are then conducted to evaluate effectiveness of the robot and gaits to portray these emotions.

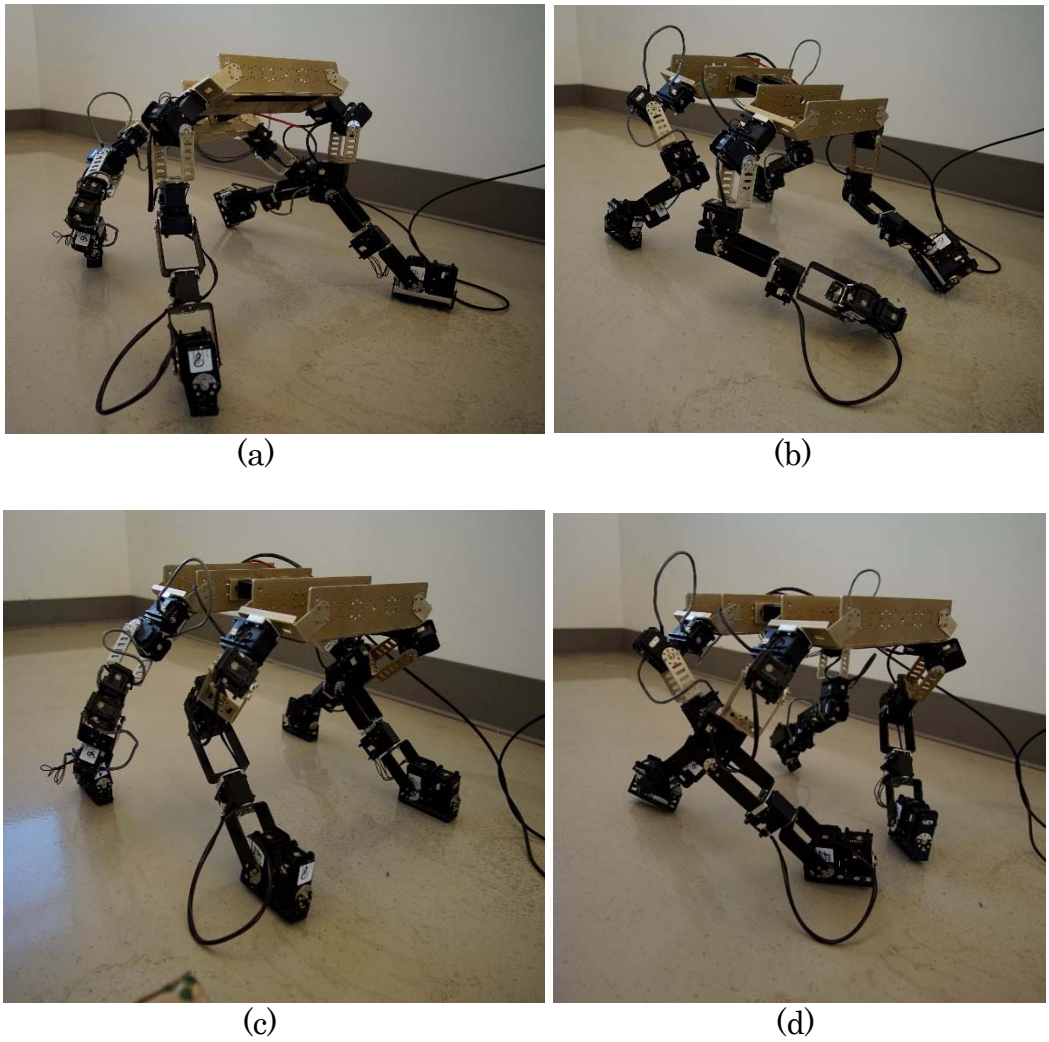

(a) (b)

(c) (d)

Figure 1. The robot displays its four emotive poses: (a) a happy pose, (b) a sad pose, (c) an angry pose, and (d) a fearful pose.

Related Work

There has been significant work studying the emotions of humans and their fellow human's abilities to interpret these emotions [5-9]. It has been evident early on that by using a human's facial cues, emotions are readily perceived. This has been supported in many studies and these facial cues are universal across world cultures [7]. The emotional categories are often split

into Ekman's six universal emotions: happy, sad, surprise, disgust, anger, fear, and often a seventh emotion is added to the list as a control variable: neutral [3, 4, 10]. There has also been work studying perception of emotions from human gaits and this has been done in many different fields of study from dance to psychology [5, 11]. These studies show that emotions of a walking human can be detected based on their gaits.

This work regarding emotional identification of humans has also been expanded into the animal kingdom [8], though it hasn't been explored as deeply as the human counterpart. For instance, based on the tonality of a dog's bark, subjects have been found to be capable of consistently identifying the dog's emotion or situation [10]. Similarly, viewing photographs of a dog's face has allowed humans (both those experienced with dogs and those with minimal dog interaction) to identify the dog's emotional state, again using Ekman's six emotions (plus neutral) [12]. When comparing the facial muscles of humans to dogs, there are many strong correlations, inferring that this ability to determine a dog's emotion based on its face are kinesthetically appropriate [13]. Darwin describes the actions and body posture of dogs in emotional states or situations in detail [8], but no work has been found that explicitly examines a dog's gait in relation to its emotions.

In order to study *emotive* gaits, the gaits themselves need to be studied and the gaits of mammalian quadrupeds happen to be well documented [14, 15]. At this point, though, there is no research surrounding a canine's or a

similar living quadruped's emotion or situation based solely on their gait.

Meanwhile, to improve human robot interaction, studies are being done to mimic human emotions utilizing robots. By creating articulated faces on robotic platforms, users can successfully identify intended displays of emotions similar to the emotional facial recognition of humans mentioned above [16, 17]. In addition, robots have imitated actors setting down a cup as well as imitating knocking on a door in different emotive states [18]. The emotive human gait has also been parameterized and transferred to a hexapod in an effort to produce robotic emotive gaits, though its effectiveness was never evaluated [19]. Additional human gait parameterization based on emotions has been gathered with the intent to improve human robot interaction; however, these parameters were never applied to a robotic system [3].

Quadrupedal gaits have been well studied in many different facets. The stability of static gaits has been well documented [20]. Quadrupedal gaits have also been shown to handle rough terrain, often by employing cost functions [21]. Not only have static gaits been well explored, but quadrupedal dynamic gaits are also a growing field in research [22]. In addition to these gait studies, robotic dogs are capable of displaying emotions by utilizing movement of the head and tail while walking [2]. Little other research has been done regarding the emotional display of a quadruped robot though.

Robots have also been shown to have positive effects in therapy

sessions with children diagnosed with autism [1]. There are also suggestions that, with children diagnosed with autism, a mobile robot could be used as a cognitive orthotic or safety blanket. This suggests that combining emotional therapy with a mobile robot has the potential to significantly impact autistic therapy [23].

All of these studies can be brought together and expounded upon to create a quadruped robot that can walk in such a manner that a human will perceive it as emotional. This will be done using the gait of the robot alone; there will be no superfluous indicators such as a head, tail, or bristling fur.

Contributions

This thesis makes several contributions related to using robots to display emotions through their body language. Subject studies demonstrate that Mr. Pete is effective in displaying happiness, fear, and anger, but sadness is sometimes misinterpreted. As indicated in the related work, this has not been accomplished previously with quadrupedal robots. To accomplish this goal, this research contributes methods of generating poses sufficient to elicit emotions and contributes poses for neutral, happy, sad, fear, and anger. While the initial emotional poses were based upon intuition and imagery of dogs and cats from the internet, this research contributes subject studies to adapt the poses to make them more convincing. Towards achieving emotional gaits, we propose to overlay the emotional poses on top of

the neutral pose to represent the emotions as a deviation from the neutral pose. Standard gait generation is applied to create the neutral gait, but this work highlights that the emotional poses must be modified such that a stable emotional gait is created. The research also contributes results that prove that the proposed redundant leg design is sufficient for creating these emotive gaits as well as methods for dealing with inverse kinematics such that the emotions are consistently portrayed throughout the gait. The research also provides a method for computing the inverse of Euler's finite rotation formula, which is necessary in solving for the inverse kinematics.

Thesis Outline

The majority of the technical developments necessary to realize this work are presented in Chapter 2, where methods are presented. Design of the robot and legs is presented first, followed by inverse kinematics and methods of providing consistent leg configurations. The central pattern generator is shown, following the inverse kinematics, which details the realization of the gaits. The central pattern generator includes the creation of leg trajectories, application of the inverse kinematics, inverse dynamic solving, and methods for balancing the robot throughout its various emotional gaits. Following the explanation of the central pattern generator, the method for creation of the emotional poses/key frames is presented, along with the final resulting emotional poses. The last detail concerning methods

regards overlaying these poses atop a neutral gait and details the necessary considerations for ensuring a stable emotional gait.

Chapter 3 discusses the study designs used for universalizing the emotive gaits and evaluating their effectiveness, and Chapter 4 details these studies. Evaluation of the results can be seen in Chapter 5, including the rejection of the null hypothesis with a chi-squared independence test.

There is still much work that can be done despite the successes discussed in Chapter 5; suggestions regarding future work are given in Chapter 6. All of this work is summarized in Chapter 7, the conclusion, and is followed by three appendices. The first appendix formalizes the inverse solving of Euler's finite rotation formula. This work is utilized multiple times in the solving of the inverse kinematics. Appendix B provides the C++ code that was used for the real-world application of the inverse kinematics and finally, Appendix C gives the IRB approval letter.

2. METHODS

In order to realize emotive gaits, this work show a method for designing and creating a walking robot that can be summarized by a few distinct components, beginning with the physical design and construction of the robot along with a simulation of the robot. With the structure of the robot in place, it is shown how to determine this robot's forward and inverse kinematics; also of importance, the singularities and limitations of the robot's workspace are addressed. These components allow for a central pattern generator (CPG) to be designed that facilitates the locomotion of the robot. The CPG includes the dynamics of the robot, manipulator trajectories, and balancing. Despite these distinctions and categorization in the creation of a robotic system, it is important to realize that for an effective system to be made, each developmental section depends on every other section, so considerations of all aspects must continually be kept in mind throughout the entire design process.

One method to progress from a walking robot to an emotive walking robot is through the use of poses, or key frames, which is shown to be effective in this work. This begins with the initial position of the robot from the CPG, which is taken as a neutral pose. This neutral pose is then altered

and displayed in a manner such that it now displays each desired emotion. This displacement can be thought of as an overlay, and applying these various pose overlays to the CPG leads to the creation of the emotive gaits by maintaining the pose displacements throughout the entire gait.

Build and Design of Robot

When designing a quadruped with the purpose of displaying emotions, as in the case of this research, it is desirable for the legs to have significant mobility and reconfigurability. By so doing, the robot will have immense freedom to orient its body and alter the form of the legs throughout the gait. With this in mind, a quadruped was designed with seven degrees of freedom (DOF) in each leg, resulting in a twenty-eight DOF robot. With a typical six DOF leg, the foot/end effector can have both its position and its orientation defined, but by adding an addition joint, the leg becomes redundant, and in turn, reconfigurable. This reconfigurability is what allows for the legs themselves to enter specific postures throughout the gait, and allows the leg freedom beyond mere locomotion; such as eliciting emotions.

The final leg design was chosen to have a spherical shoulder/hip, a single joint in the knee, and a spherical ankle, which can be seen in Figure 2. This configuration puts the redundancy of the seven DOF leg in the orientation of the knee. By having the redundancy in the angle of knee relative to the body, the robot is capable of changing its apparent width as

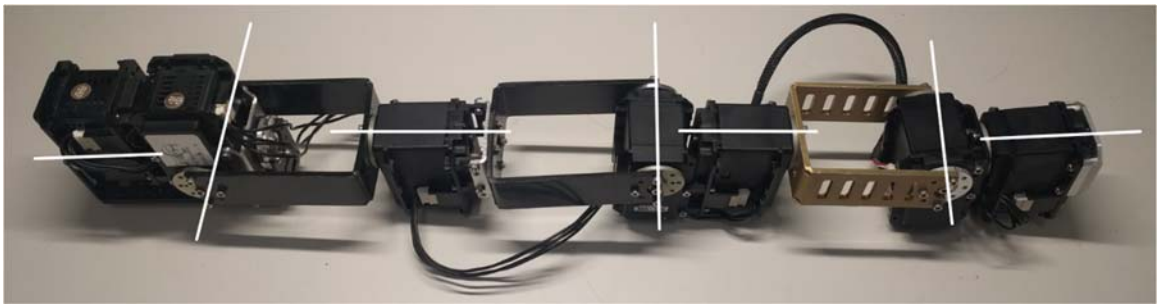

Figure 2. Photograph of the leg's zero angle configuration. Each servo's joint axis has been highlighted in white. The left end corresponds to the leg's foot, and the right end is the mounting point to the body.

seen in Figure 1, this changing of width can be seen in nature with different emotive applications such as a gorilla widening its stance to appear dominant or a dog cowering in fear.

The legs of the robot were attached to the body at a forty-five-degree angle below the robot's x-y plane, which can be seen in Figure 3. This was suggested based on unpublished research from Kairos Autonomi in order to increase the leg's available workspace below the robot. Ideally the robot would have a perfect sphere of workable space; unfortunately, because of the limitations imposed by physical hardware, this cannot occur. Since the purpose of the robot is to walk, workspace below the robot's x-y plane should be prioritized.

This robot was designed such that when in a completely upright pose, the body is 50cm from the ground, and the body was designed to be 25cm wide and 35cm long. These dimensions were based on available hardware and a goal of trying to maintain a visually proportionate robot. The robot,

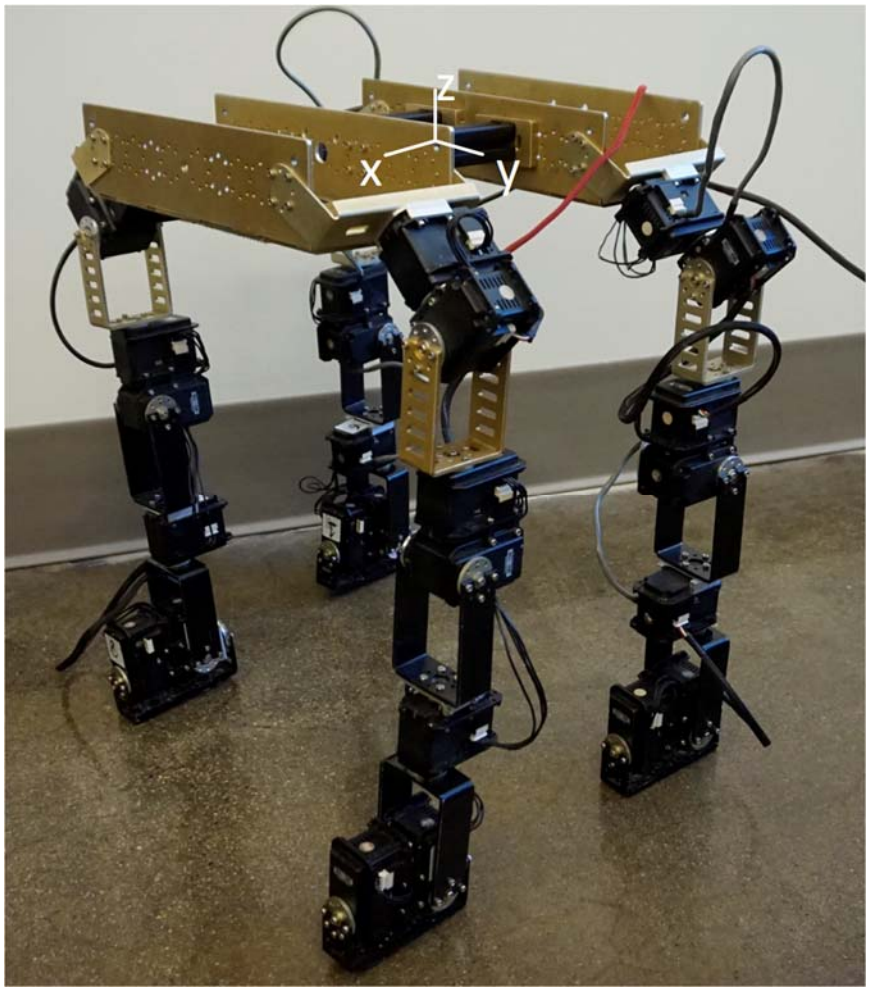

Figure 3. Image of the 28 degree of freedom quadruped. The robot's reference frame is shown in white and is centered in the robot's body.

constructed from servo motors, can be seen in Figure 3 where it may be noted that no covering or skin was placed on the robot. This was done intentionally to refrain from superfluous physical additions and to ensure that any perceived emotions were based on the gait of the robot and not its static physical appearance. This robot was also simulated in the Virtual Robotics Experimentation Platform (VREP), and the simulated robot can be seen in Figure 4.

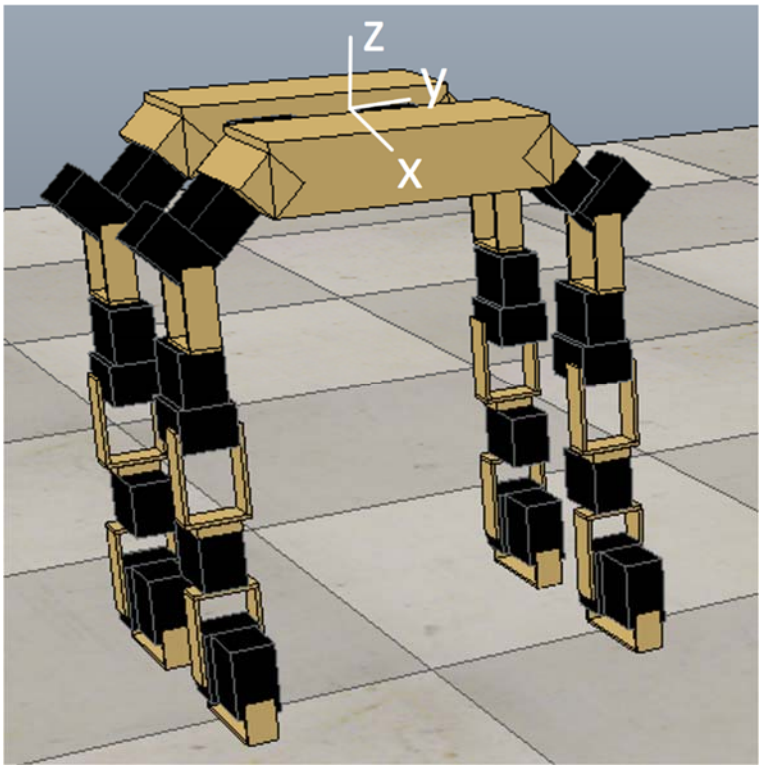

Figure 4. Image of the quadruped simulated in the Virtual Robotics Experimentation platform. The robot's reference frame is shown in white and is centered in the robot's body.

Inverse Kinematics

A major benefit to the legs being designed with two spherical joints separated by a 1 DOF knee is that a closed form solution to the inverse kinematics can be solved for. From the robot's reference frame, each foot is given a goal position, orientation, and a goal angle for its elbow: the robot's reference frame is defined as positive x pointing toward the front of the robot body, positive y pointing toward the left of the robot body, positive z pointing towards the top of the robot body, and the reference frame is centered in the

robot's body, which is highlighted in Figure 3. Every leg has an identical kinematic structure, so with a knowledge of the geometry of the robot, the same inverse kinematics solution can be used for each leg.

Each leg was designed to have the structure of a 6R arm, but with an additional joint between the 2nd and 3rd joint when counting from the proximal end of the 6R arm (in this case the shoulder/hip) as seen in Figure 5 with the DH parameters described in Table 1. Such a design leads to an over-constrained system with regards to a desired tool frame position and orientation, so to solve for the inverse kinematics, task space augmentation can be incorporated by also specifying a desired angle for the elbow in relation to the body [24]. A similar arm is described in [25] and the joint angles can be solved for in the same order as proposed there, but for an accurate solution that leads to the desired end effector position and orientation, as well as the desired elbow angle, different functions must be

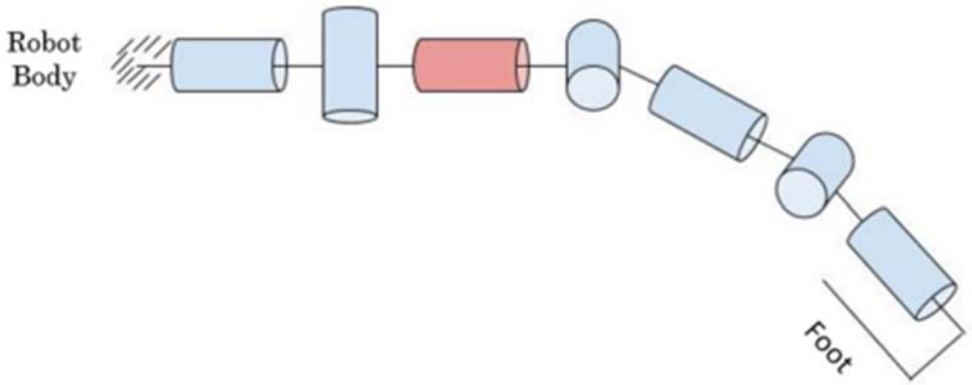

Figure 5. Depiction of the modified 6R arm, with the added link highlighted in red. In this application, the base frame is located on the robot's body and the typical end effector is the quadruped's foot. The joints rotate along each cylinder's axis.

Table 1: DH parameters of the 7 DOF serial, rotary manipulator used for each leg of the quadruped.

i	$\boldsymbol{a_i}$	$\boldsymbol{d_i}$	$\boldsymbol{\alpha_i}$
1	0	0	$\pi/2$
2	0	0	$\pi/2$
3	0	d_3	$-\pi/2$
4	0	0	$\pi/2$
5	0	d_5	$-\pi/2$
6	0	0	$\pi/2$
7	0	0	0

used to solve for each joint angle. This is because of differences in the task space augmentation definitions and to ensure consistent leg configurations throughout each leg's trajectory.

Starting from the body of the robot, the desired position and orientation of the foot is transformed such that they are now located at the proximal end of the leg (the shoulder/hip) and describe the position and orientation of the ankle (referred to as the wrist in terms of the 6R arm):

$$^{robot}\boldsymbol{T}_{foot} = \begin{bmatrix} ^{robot}\boldsymbol{R}_{foot} & ^{robot}\boldsymbol{p}_{foot} \\ \boldsymbol{0}^T & 1 \end{bmatrix}$$

$$^{0}\boldsymbol{T}_{ankle} = (^{robot}\boldsymbol{T}_0)^{-1} * {}^{robot}\boldsymbol{T}_{foot} * \left(^{ankle}\boldsymbol{T}_{foot}\right)^{-1}$$

where $^{robot}\boldsymbol{T}_0$ and $^{ankle}\boldsymbol{T}_{foot}$ are known from the robot's geometry. The angle of the fourth joint can immediately be found now that the position of the ankle, $\boldsymbol{p}_a$, is known:

$$\theta_4 = \pm\text{atan}\left(\frac{\sqrt{(d_3+d_5)^2 - |\boldsymbol{p}_a|^2}}{|\boldsymbol{p}_a|^2 - (d_3+d_5)^2}\right)$$

This results in two solutions, commonly known as the elbow-in and elbow-out

configurations. To maintain the rear knees bending toward the front of the robot, the negative solution should be utilized, and to maintain the front knees bending toward the rear of the robot, the positive solution should be utilized, the result of which is shown in Figure 6. This results in matching knee orientations of both canines and felines. At this point, the first two joint angles must be solved for as if the redundant joint was nonexistent (or equivalently, $\theta_3 = 0$):

$$\theta_1' = \operatorname{atan2}(\boldsymbol{p}_a(1), \boldsymbol{p}_a(0))$$

$${}^1\boldsymbol{p}_a' = \begin{bmatrix} \cos(t_1') & 0 & \sin(t_1') \\ \sin(t_1') & 0 & -\cos(t_1') \\ 0 & 1 & 0 \end{bmatrix}^T * \boldsymbol{p}_a$$

$$\phi = \operatorname{atan2}({}^1\boldsymbol{p}_a'(1), {}^1\boldsymbol{p}_a'(0))$$

$$\psi = \operatorname{atan2}(d_5 \sin(t_4)\ , d_3\ +\ d_5 \cos(t_4))$$

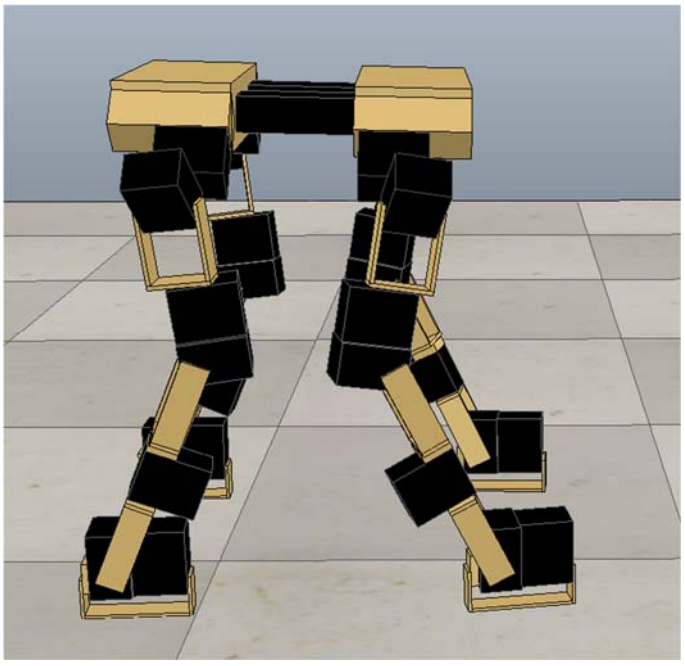

Figure 6. The robot is designed to have both knees pointed in. This is the same orientation as a canine or feline.

$$\theta_2' = \phi - \psi + \frac{\pi}{2}$$

where the prime notation indicates the solution when $\theta_3 = 0$. Traditionally, the four-quadrant arc tangent function is not utilized in the solving for t_1' and two solutions exist corresponding to two separate and opposite shoulder configurations; however, in this application, the four-quadrant arc tangent function leads to consistency throughout the manipulator's trajectory. The position of the elbow without any rotation can then be found:

$$\boldsymbol{p_e'} = \begin{bmatrix} d_3\cos(\theta_1')\sin(\theta_2') \\ d_3\sin(\theta_1')\sin(\theta_2') \\ -d_3\cos(\theta_2') \end{bmatrix}$$

Then, using Euler's finite rotation equation [26], the position of the elbow can be rotated by the desired elbow angle to its final position:

$$\boldsymbol{n'} = \frac{\boldsymbol{p_e'}}{|\boldsymbol{p_e'}|}$$

$$\boldsymbol{p}_e = \boldsymbol{n'} * \boldsymbol{n'} \cdot \boldsymbol{p_e'} * (1 - \cos(\theta_e)) + \boldsymbol{p_e'} * \cos(t_e) + \boldsymbol{n'} \times \boldsymbol{p_e'} * \sin(\theta_e)$$

Now that the location of the elbow is known, the first two joint angles may now be solved for uniquely:

$$\theta_1 = \text{atan2}(\boldsymbol{p}_e(1), \boldsymbol{p}_e(0))$$

$$\theta_2 = \text{atan2}(\sqrt{\boldsymbol{p}_e(0)^2 + \boldsymbol{p}_e(1)^2}, -\boldsymbol{p}_e(2))$$

Then, by utilizing the inverse of Euler's finite rotation equation (which is detailed in Appendix A) the redundant third joint angle may be found, but first the supporting vectors must be defined as well as the position of the wrist if the redundant joint were nonexistent:

$$ {}^{0}\boldsymbol{T}'_{5} = {}^{0}\boldsymbol{T}_{1}\,{}^{1}\boldsymbol{T}_{2}\,{}^{2}\boldsymbol{T}'_{3}\,{}^{3}\boldsymbol{T}_{4}\,{}^{4}\boldsymbol{T}'_{5} $$

$$ \boldsymbol{p}'_{a} = \begin{bmatrix} {}^{0}\boldsymbol{T}'_{5}(0,3) \\ {}^{0}\boldsymbol{T}'_{5}(1,3) \\ {}^{0}\boldsymbol{T}'_{5}(2,3) \end{bmatrix} $$

$$ \boldsymbol{p}'_{ea} = \boldsymbol{p}'_{a} - \boldsymbol{p}_{e} $$

$$ \boldsymbol{p}_{ea} = \boldsymbol{p}_{a} - \boldsymbol{p}_{e} $$

$$ \boldsymbol{n} = \frac{\boldsymbol{p}_{e}}{|\boldsymbol{p}_{e}|} $$

Note that the transformation from the base of the robot to the supplemental wrist location, ${}^{0}\boldsymbol{T}'_{5}$, relies on θ_5, which has not yet been solved for. However, θ_5 does not affect the supplemental wrist position ($\boldsymbol{p}'_{w}$), only its orientation, and in order to solve for θ_3, we only need the wrist's position; so for now, an arbitrary, temporary value for θ_5 may be chosen. With these vectors defined, the inverse of the finite rotation formula may now be applied:

$$ \cos(\theta_3) = \frac{\boldsymbol{p}'_{ea} \cdot \boldsymbol{p}_{ea} - \boldsymbol{p}'_{ea} \cdot \boldsymbol{n} * (\boldsymbol{n} \cdot \boldsymbol{p}'_{ea})}{\boldsymbol{p}'_{ea} \cdot \boldsymbol{p}'_{ea} - \boldsymbol{p}'_{ea} \cdot \boldsymbol{n} * (\boldsymbol{n} \cdot \boldsymbol{p}'_{ea})} $$

$$ \sin(\theta_3) = \frac{(\boldsymbol{n} \times \boldsymbol{p}'_{ea}) \cdot (\boldsymbol{p}_{ea} - \boldsymbol{n} * (\boldsymbol{n} \cdot \boldsymbol{p}'_{ea}))}{(\boldsymbol{n} \times \boldsymbol{p}'_{ea}) \cdot (\boldsymbol{n} \times \boldsymbol{p}'_{ea})} $$

$$ \theta_3 = \operatorname{atan2}(\sin(\theta_3), \cos(\theta_3)) $$

Finally, the last three joint angles ($\theta_5, \theta_6,$ and θ_7) can be found using the standard solution to the spherical wrist problem [27], which is described here for completeness:

Starting with the four known joint angles and the desired end effector orientation, the orientation from the base of the wrist to the end effector is easily found:

$$^4\boldsymbol{R}_a = (^0\boldsymbol{R}_1 * {}^1\boldsymbol{R}_2 * {}^2\boldsymbol{R}_3 * {}^3\boldsymbol{R}_4)^T * {}^0\boldsymbol{R}_a$$

$$^4\boldsymbol{R}_a = {}^4\boldsymbol{R}_5 * {}^5\boldsymbol{R}_6 * {}^6\boldsymbol{R}_a$$

θ_5 can be isolated by manipulating the order of transformation matrices and inspecting their individual elements:

$$^4\boldsymbol{R}_a * {}^6\boldsymbol{R}_a^T = {}^4\boldsymbol{R}_5 * {}^5\boldsymbol{R}_6$$

Multiplying the rotation matrices on each side results in:

$$^4\boldsymbol{R}_a * {}^6\boldsymbol{R}_a^T = \begin{bmatrix} r_{11} & r_{12} & r_{13} \\ r_{21} & r_{22} & r_{23} \\ r_{31} & r_{32} & r_{33} \end{bmatrix} * \begin{bmatrix} \mathrm{c}(\theta_7) & \mathrm{s}(\theta_7) & 0 \\ -\mathrm{s}(\theta_7) & \mathrm{c}(\theta_7) & 0 \\ 0 & 0 & 1 \end{bmatrix} = \begin{bmatrix} \vdots & \vdots & r_{13} \\ \vdots & \vdots & r_{23} \\ \vdots & \vdots & r_{33} \end{bmatrix}$$

$$^4\boldsymbol{R}_5 * {}^5\boldsymbol{R}_6 = \begin{bmatrix} \mathrm{c}(\theta_5) & 0 & -\mathrm{s}(\theta_5) \\ \mathrm{s}(\theta_5) & 0 & \mathrm{c}(\theta_5) \\ 0 & -1 & 0 \end{bmatrix} * \begin{bmatrix} \mathrm{c}(\theta_6) & 0 & \mathrm{s}(\theta_6) \\ \mathrm{s}(\theta_6) & 0 & -\mathrm{c}(\theta_6) \\ 0 & 1 & 0 \end{bmatrix} = \begin{bmatrix} \vdots & \vdots & \mathrm{s}(\theta_6) * \mathrm{c}(\theta_5) \\ \vdots & \vdots & \mathrm{s}(\theta_6) * \mathrm{s}(\theta_5) \\ \vdots & \vdots & \mathrm{c}(\theta_6) \end{bmatrix}$$

where θ_5 can now be solved for:

$$\theta_5 = \tan^{-1}\left(\frac{\mathrm{s}(\theta_5) * \mathrm{s}(\theta_6)}{\mathrm{c}(\theta_5) * \mathrm{s}(\theta_6)}\right) = \tan^{-1}(\frac{r_{23}}{r_{13}})$$

This results in two separate solutions for θ_5, but again, for consistency throughout the portion of the workspace within which the foot operates, the four-quadrant arctangent function should be utilized:

$$\theta_5 = \mathrm{atan2}(r_{23}, r_{13})$$

θ_6 and θ_7 can be uniquely defined with a similar approach:

$$^4\boldsymbol{R}_5^T * {}^4\boldsymbol{R}_a = {}^5\boldsymbol{R}_6 * {}^6\boldsymbol{R}_a$$

Multiplying the rotation matrices on each side results in:

$$^4\boldsymbol{R}_5^T * {}^4\boldsymbol{R}_a = \begin{bmatrix} \mathrm{c}(\theta_5) & s(\theta_5) & 0 \\ 0 & 0 & -1 \\ -\mathrm{s}(\theta_5) & \mathrm{c}(\theta_5) & 0 \end{bmatrix} * \begin{bmatrix} r_{11} & r_{12} & r_{13} \\ r_{21} & r_{22} & r_{23} \\ r_{31} & r_{32} & r_{33} \end{bmatrix}$$

$$= \begin{bmatrix} \vdots & \vdots & r_{13}\mathrm{c}(\theta_5) + r_{23}\mathrm{s}(\theta_5) \\ \vdots & \vdots & -r_{33} \\ -r_{11}\mathrm{s}(\theta_5) + r_{21}c(\theta_5) & -r_{12}\mathrm{s}(\theta_5) + r_{22}\mathrm{c}(\theta_5) & -r_{13}\mathrm{s}(\theta_5) + r_{23}\mathrm{c}(\theta_5) \end{bmatrix}$$

$${}^5\boldsymbol{R}_6 * {}^6\boldsymbol{R}_a = \begin{bmatrix} \vdots & \vdots & \mathrm{s}(\theta_6) \\ \vdots & \vdots & -\mathrm{c}(\theta_6) \\ \mathrm{s}(\theta_7) & \mathrm{c}(\theta_7) & 0 \end{bmatrix}$$

where θ_6 and θ_7 can now be found:

$$\theta_6 = \mathrm{atan2}\big(\mathrm{s}(\theta_6), \mathrm{c}(\theta_6)\big) = \mathrm{atan2}(r_{13}\mathrm{c}(\theta_5) + r_{23}\mathrm{s}(\theta_5),\ r_{33})$$

$$\theta_7 = \mathrm{atan2}\big(\mathrm{s}(\theta_7), \mathrm{c}(\theta_7)\big) = \mathrm{atan2}(-r_{11}\mathrm{s}(\theta_5) + r_{21}\mathrm{c}(\theta_5), -r_{12}\mathrm{s}(\theta_5) + r_{22}\mathrm{c}(\theta_5))$$

To summarize, by utilizing task space augmentation, each joint angle can be solved for with a vigorous closed form solution – vigorous in the sense that it can maintain desired configurations throughout the entire end effector trajectory despite multiple solutions being possible. This requires a desired foot position and orientation, as well as an angle relating the knee to the body. By using these inverse kinematics, not only is locomotion possible, but each individual leg's posture can be modified throughout a gait.

Inverse Kinematic Consistencies

It is important to note that there are three separate potential singularities in the solution of the inverse kinematics: when $\theta_6 = 0\ or\ \pi$ (the wrist singularity), when $\theta_4 = 0\ or\ \pi$ (the knee singularity), and when $\theta_2 = 0\ or\ \pi$ (the shoulder singularity). In each of these singularities, the preceding joint angle can be set to 0 and the following joint can be solved as usual. In addition to considering singularities, the configuration of the knee must be

maintained because at times, it will attempt to switch from elbow-in to elbow-out, or vice versa. This maintenance is done with a recursive solution of the inverse kinematics based on the previous position of the elbow and the previous position of the ankle, and an intelligent application of dot and cross products.

This novel maintenance is done by taking the cross product of the old elbow position with the old ankle position and comparing that to the cross product of the proposed elbow position with the proposed ankle position. By doing this, it is possible to tell if the vectors are pointing into or out of the same plane. If so, then the elbow configuration is the same. If they are in opposing directions, then the elbow configurations are different and the inverse kinematics must be resolved with an addition of π to the desired elbow angle.

This can be stated in mathematical terms as follows:

$$if\ \left(\boldsymbol{p}_{e,old} \times \boldsymbol{p}_{a,old}\right) \cdot \left(\boldsymbol{p}_e \times \boldsymbol{p}_a\right) < 0 \quad : \quad \theta_e \mathrel{+}= \pi$$

By adding π to θ_e, the knee will be rotated into the desired configuration. This checking algorithm as well as the inverse kinematics have been implemented in C++ code that is detailed in Appendix B.

Central Pattern Generator

With a closed form solution to the inverse kinematics in place, a central pattern generator is ideal for creating an initial neutral gait, establishing the necessary prerequisite for emotive gait experimentation. In the proposed approach, a neutral gait is made first before emotive gaits are created. For this application, a crawl was chosen from the creep style of gaits with a duty factor of $\beta = 0.75$, which is the fastest possible quasi-static gait for a quadruped [28, 29]. While more dynamic gaits are possible in future work, this gait was chosen for its simplicity and to evaluate its ability to demonstrate emotional display. The creep style of gait has also been shown to be the preferred gait in mammals when it is available [20]. In this gait, the feet swing in the order of: {RH, RF, LH, LF}, where L stands for left, R stands for right, H stands for hind, and F stands for front. This ordering mimics the pattern that canines exhibit when walking [14].

With this CPG, the orientation of the body remains fixed throughout the gait, it also leads to a fixed velocity of the body in the x-direction and the body height remains constant. Given a desired step length and step height, the neutral pose is created by lowering the body of the robot at least to the point that a step can be made without any leg leaving its workspace. With the robot used in this study, the neutral gait was created with an 80mm step length, 40 mm step height, and the body was lowered 200 mm; this can be seen in Figure 6. A benefit of lowering the body more than the minimal

amount is that kinematic singularities are more easily avoided, however, care must be taken not to lower the body an excessive amount; recall that this initial lowering creates the neutral pose and to make an unnatural looking gait is undesirable for an emotionally neutral gait.

The trajectory of the swing foot follows half of a sine wave in the x-z plane, whose amplitude and period are both inputs to the CPG based on the desired characteristics of the gait. A sine wave was chosen over other common trajectories, such as polynomials, because of the ease of maintaining an identical height map for steps of varying lengths. Using a sine wave for this reason ensures that the initial steps of the robot will be high enough for the swing foot to lose contact with the ground even when faced with modeling errors of the robot and walking surface.

Stabilization of the gait is done with a calculation of the center of pressure (COP) [30] and is augmented with the dynamics of the swinging foot, which were calculated with the recursive Newton-Euler algorithm. The change in the COP by the computed dynamics is described by:

$$\Delta x = -\frac{\tau_y + h * F_{ex}}{F_{ez} + w}$$

$$\Delta y = \frac{\tau_x - h * F_{ey}}{F_{ez} + w}$$

where h is the current height of the robot, w is the weight of the robot, and τ and F are the computed dynamic torques and forces [29].

Only the swing foot's dynamics were taken into consideration because

ideally the robot moves at a constant velocity and the stance legs move at 1/3 of the pace of the swinging foot, and by neglecting them, significant computation time can be saved. This augmentation results in a similar balancing algorithm as the common zero moment point (ZMP) algorithm used in bipedal balancing [31] where if the COP is not located in the support polygon, the legs are moved so that the COP is in the support polygon; this is illustrated in Figure 7. In this implementation, the legs were only moved in the y direction so that the cyclical motion in the x direction that allows for forward translation of the robot was not affected by the balancing. It is important to note, however, that if large corrections to the body must be made to maintain balance, then the assumption of a constant velocity body cannot be held.

For this research, a buffer system had to be created for proper balancing to be achieved in the face of errors in the modeling of the dynamic parameters of the robot. The buffer was defined as a fraction of the support polygon (the fraction being determined experimentally), and if the COP was located inside of the support polygon, then changes were slowly and incrementally made to move the COP to the inside line of the shrunken support polygon, as illustrated in Figure 7. By moving to the inside line of the shrunken support polygon rather than moving to the center of the support polygon, the robot was still able to remain balanced, but when the swinging leg transitioned to a new foot, there was minimal change in y required to

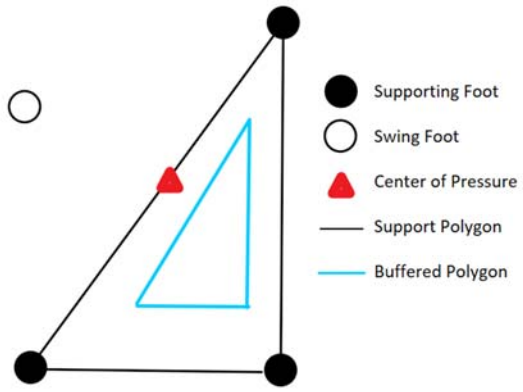

Figure 7. Illustration of the balancing method. When the center of pressure is inside of the support polygon, it is constantly moved towards the diagonal line of the buffered polygon. By doing this, there can be a mediation between the shift necessary to maintain balance when transitioning swing legs, and providing a margin of safety when balancing. If the center of pressure were outside of the support polygon, then it would immediately be shifted into it.

remain balanced and more fluid motion could be achieved.

Pose Creation

Separate from the inverse kinematics and CPG, emotive poses or key frames must be generated for each desired emotion, based on the proposed emotive gait methodology. The poses should position the robot in such a way that the posture of the body and the posture of all four legs appear to emit the desired emotion. In order for the poses to work with the CPG, they should also be symmetrical along the midsagittal plane; this symmetry allows for easy entry into the gait. Judgement regarding how an initial pose should be designed to fit a desired emotion can be done with a study of different

mammalian quadrupeds in the desired emotive states mixed with intuition. Four sample images used as inspiration to the four separate emotive poses created in this work can be seen in Figure 8 through Figure 11. Once the pose has been satisfactorily created, all that must be saved are the joint angles. Through forward kinematics, the joint angles lead to each foot's position and orientation, and the elbow of each angle in relation to the body may be found; it is each foot's location that directly defines the robot's body orientation when the robot is standing.

For convenience, each emotive pose can be described by its deviation from the neutral pose. With this definition, a pose can be represented with

Figure 8. An image of a dog used for inspiration for the happy pose. The image is from [32] with annotations added. (a) highlights the front feet being placed wider than the body, (b) shows the front legs being more extended

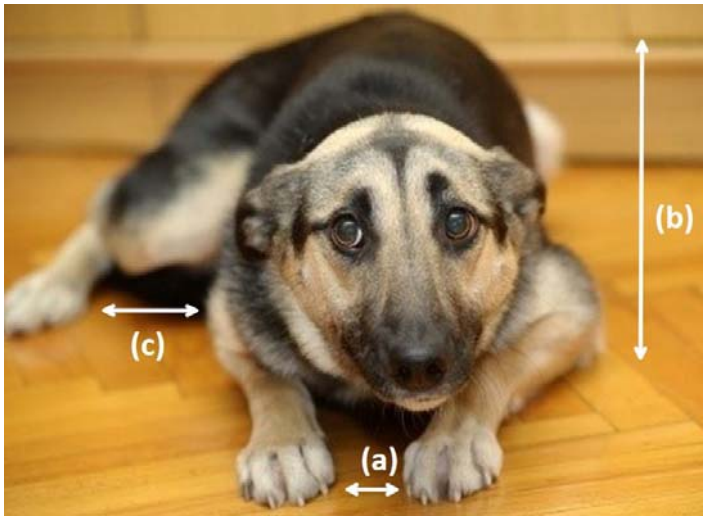

Figure 9. An image of a dog used for inspiration for the sad pose. The image is from [33] with annotations added. (a) highlights the front feet being placed on the inside of the body, (b) shows a very low overall body height, and (c) shows the rear legs being wider than the front legs.

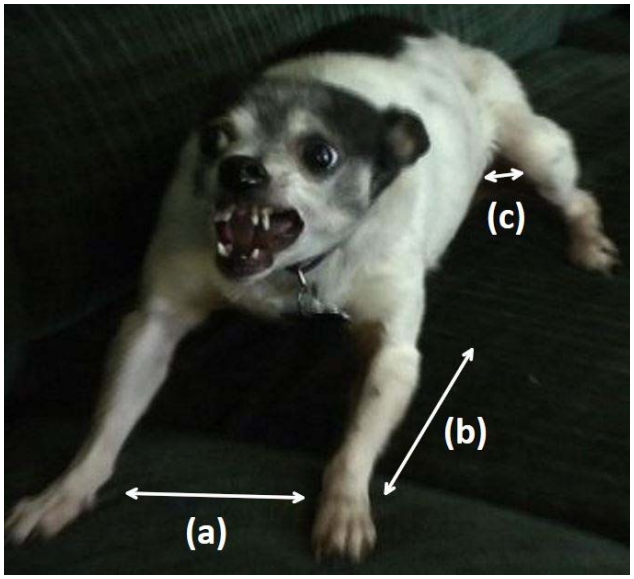

Figure 10. An image of a dog used for inspiration for the angry pose. The image is from [34] with annotations added. (a) highlights the front legs being wider than the body as well as extended in front of the body (b), and (c) shows the rear knees being rotated to extend past the body.

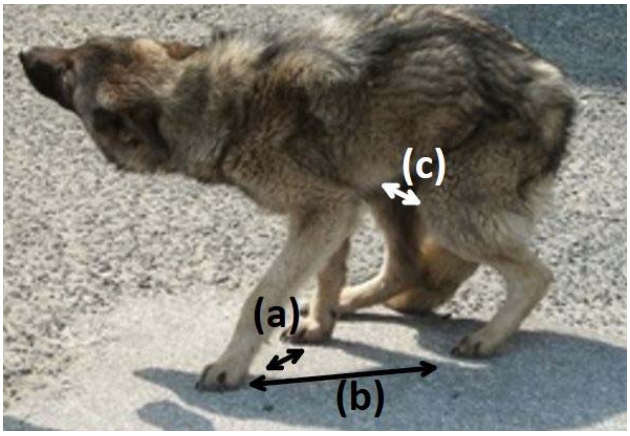

Figure 11. An image of a dog used as inspiration for the fearful pose. The image is from [35] with annotations added. (a) shows a very narrow stance in the front feet, (b) highlights how close the rear feet are to the front feet, and (c) shows how the knees are located very close together.

the variables $\{\partial \boldsymbol{p}_{FL},\ \partial \boldsymbol{R}_{FL}, \partial\theta_{FL},\ \partial \boldsymbol{p}_{HL},\ \partial \boldsymbol{R}_{HL},\ \partial\theta_{FL}, s\}$, where $\partial \boldsymbol{p}_{FL}$ is the front left foot's deviation from the neutral pose, $\partial \boldsymbol{R}_{FL}$ is the deviation of the front left foot's orientation from neutral (which can also be recorded in Euler angles), and $\partial\theta_{FL}$ is the deviation in angle of the front left knee relative to the body. The same relative parameter definitions apply to the hind left foot $(\partial \boldsymbol{p}_{HL}, \partial \boldsymbol{R}_{HL}, \partial\theta_{FL})$. Only the left side of the body is defined due to the pose's symmetry. The final variable, s, defines the speed factor that determines the robot's forward velocity. The convenience of describing each pose relative to neutral will become evident in the next section, *Emotional Overlays*. The neutral pose is described in Table 2 and Figures 12 and 13. The pose for happy is seen in Table 3, Figure 14, and Figure 15, and sadness is shown in Table 4, Figure 16, and Figure 17. Anger and Fear can be seen in Table 5, Figure 18, Figure 19, and Table 6, Figure 20, and Figure 21, respectively.

Table 2. The task space definition of the neutral pose. These parameters are with respect to the robot's reference frame. Speed factor dictates how fast the CPG should execute the pose.

	X	Y	Z
Front Left Foot Position (mm)	150	200	-300
Front Left Foot Euler Angles (rad)	0	0	0
Front Left Foot Elbow Angle (rad)	$-\frac{\pi}{2}$		
Hind Left Foot Position (mm)	-130	200	-300
Hind Left Foot Euler Angles (rad)	0	0	0
Hind Left Foot Elbow Angle (rad)	$\frac{\pi}{2}$		
Speed Factor	1		

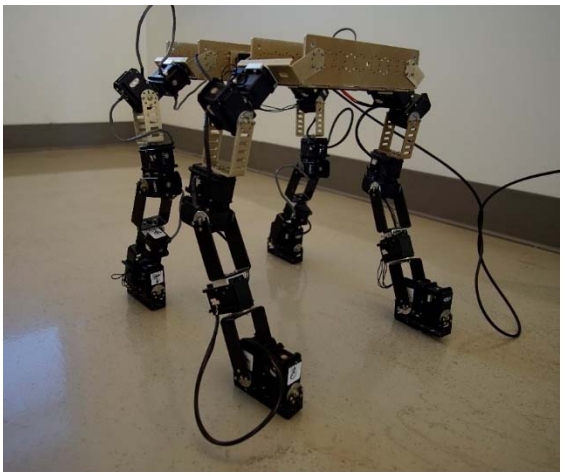

Figure 12. The initial pose of the neutral gait on the real robot.

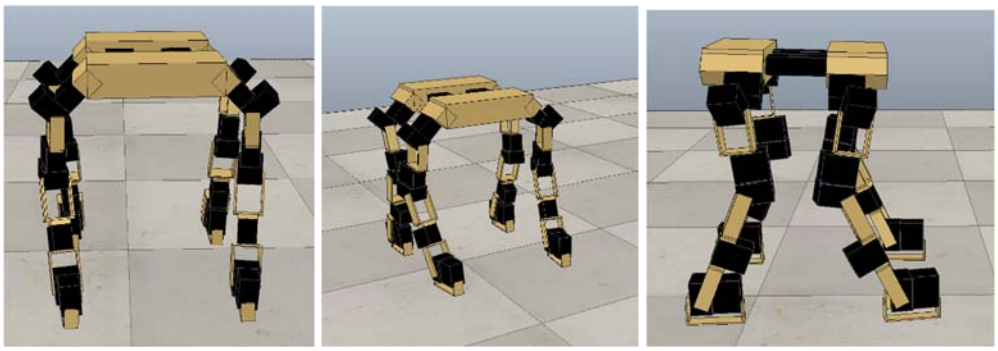

Figure 13. Depiction of the initial position of the neutral gait in simulation.

Table 3. The deviations from neutral to obtain a happy pose. These changes are with respect to the robot's reference frame. Speed factor dictates how fast the CPG should execute the pose.

	Deviation from Neutral		
	X	Y	Z
Front Left Foot Position ($\partial \boldsymbol{p}_{FL}$) (mm)	-45.6	46	10.3
Front Left Foot Euler Angles ($\partial \boldsymbol{R}_{FL}$) (rad)	1.582	0.376	1.795
Front Left Foot Elbow Angle ($\partial \theta_{FL}$) (rad)	-0.371		
Hind Left Foot Position ($\partial \boldsymbol{p}_{HL}$) (mm)	-91	27.4	161.5
Hind Left Foot Euler Angles ($\partial \boldsymbol{R}_{HL}$) (rad)	3.071	0.929	2.942
Hind Left Foot Elbow Angle ($\partial \theta_{HL}$) (rad)	-1.217		
Speed Factor (s)	0.9		

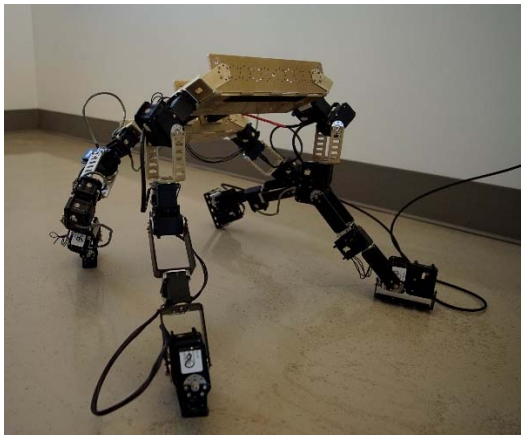

Figure 14. Image of the physical robot in the happy pose.

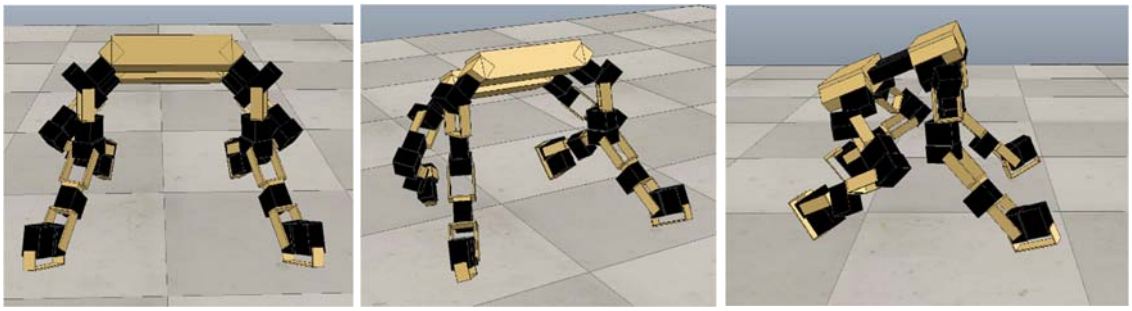

Figure 15. Images of the simulated robot in the happy pose.

Table 4. The deviations from neutral to obtain a sad pose. These changes are with respect to the robot's reference frame. Speed factor dictates how fast the CPG should execute the pose.

	Deviation from Neutral		
	X	Y	Z
Front Left Foot Position ($\partial \boldsymbol{p}_{FL}$) (mm)	82.9	-19.8	108.8
Front Left Foot Euler Angles($\partial \boldsymbol{R}_{FL}$) (rad)	-1.917	0.809	-1.949
Front Left Foot Elbow Angle ($\partial \theta_{FL}$) (rad)	0.961		
Hind Left Foot Position ($\partial \boldsymbol{p}_{HL}$) (mm)	8.4	9.1	62.3
Hind Left Foot Euler Angles ($\partial \boldsymbol{R}_{FL}$) (rad)	-0.463	0.631	-2.239
Hind Left Foot Elbow Angle ($\partial \theta_{FL}$) (rad)	0.187		
Speed Factor (s)	0.5		

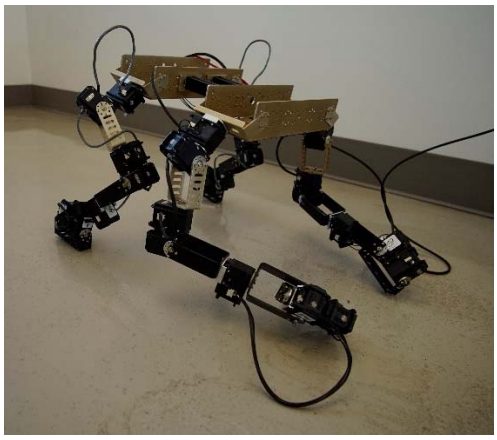

Figure 16. Image of the physical robot in the sad pose.

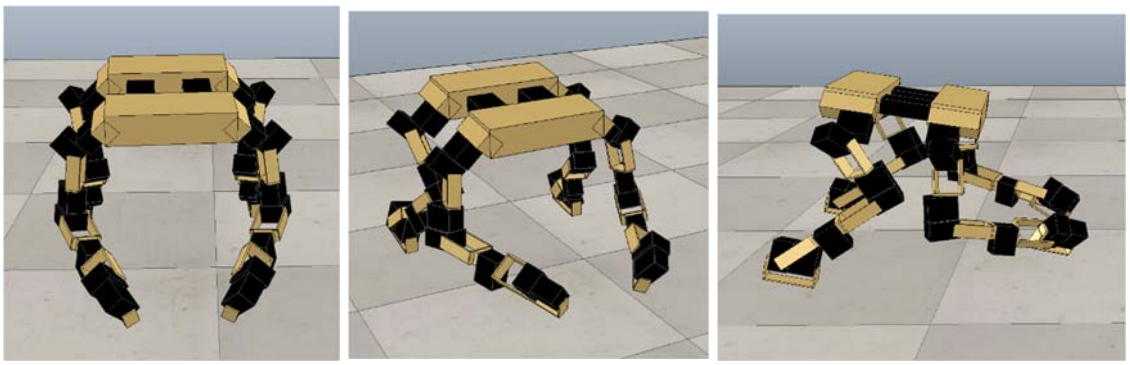

Figure 17. Images of the simulated robot in the sad pose.

Table 5. The deviations from neutral to obtain an angry pose. These changes are with respect to the robot's reference frame. Speed factor dictates how fast the CPG should execute the pose.

	Deviation from Neutral		
	X	Y	Z
Front Left Foot Position ($\partial \boldsymbol{p}_{FL}$) (mm)	-45.3	-2.8	80.4
Front Left Foot Euler Angles ($\partial \boldsymbol{R}_{FL}$) (rad)	0.942	-0.125	-1.571
Front Left Foot Elbow Angle ($\partial \theta_{FL}$) (rad)	-0.203		
Hind Left Foot Position ($\partial \boldsymbol{p}_{HL}$) (mm)	-15.5	83.9	66.7
Hind Left Foot Euler Angles ($\partial \boldsymbol{R}_{FL}$) (rad)	0	-1.116	-1.571
Hind Left Foot Elbow Angle ($\partial \theta_{FL}$) (rad)	-0.986		
Speed Factor (s)	1.5		

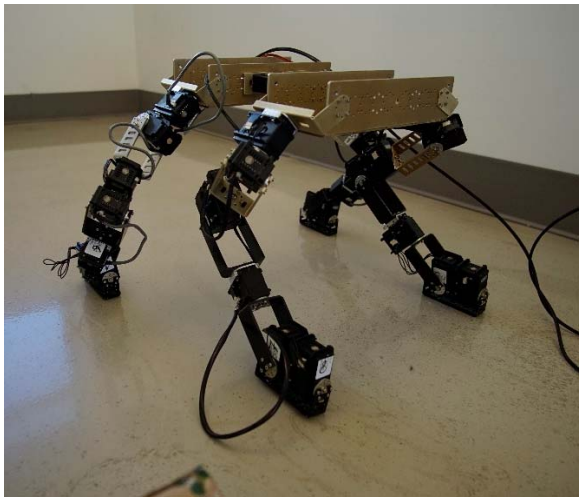

Figure 18. Image of the physical robot in the angry pose.

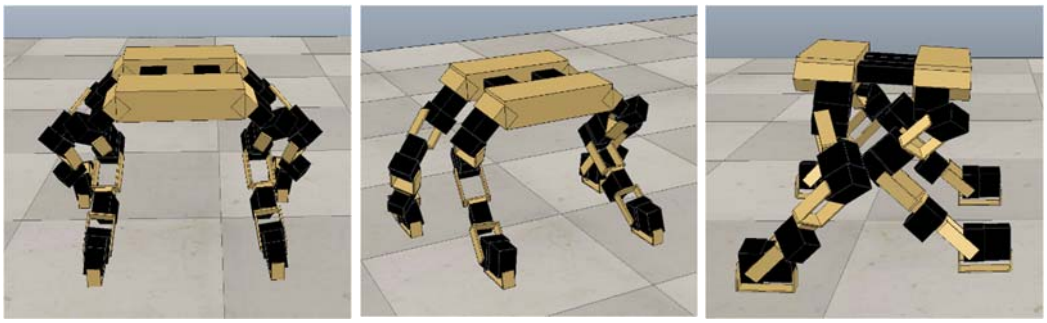

Figure 19. Images of the simulated robot in the angry pose.

Table 6. The deviations from neutral to obtain a fearful pose. These changes are with respect to the robot's reference frame. Speed factor dictates how fast the CPG should execute the pose. In this case, a negative speed factor indicates backing up.

	Deviation from Neutral		
	X	Y	Z
Front Left Foot Position ($\partial \boldsymbol{p}_{FL}$) (mm)	-63.4	-45.8	55.4
Front Left Foot Euler Angles ($\partial \boldsymbol{R}_{FL}$) (rad)	-1.671	-0.287	-1.861
Front Left Foot Elbow Angle ($\partial \theta_{FL}$) (rad)	0.456		
Hind Left Foot Position ($\partial \boldsymbol{p}_{HL}$) (mm)	-55.7	-12.4	72.4
Hind Left Foot Euler Angles ($\partial \boldsymbol{R}_{FL}$) (rad)	2.011	0.693	-2.025
Hind Left Foot Elbow Angle ($\partial \theta_{FL}$) (rad)	0.137		
Speed Factor (s)	-0.5		

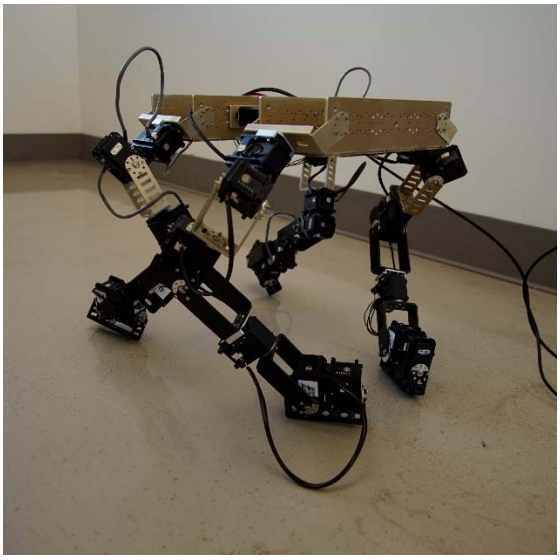

Figure 20. Image of the physical robot in the fearful pose.

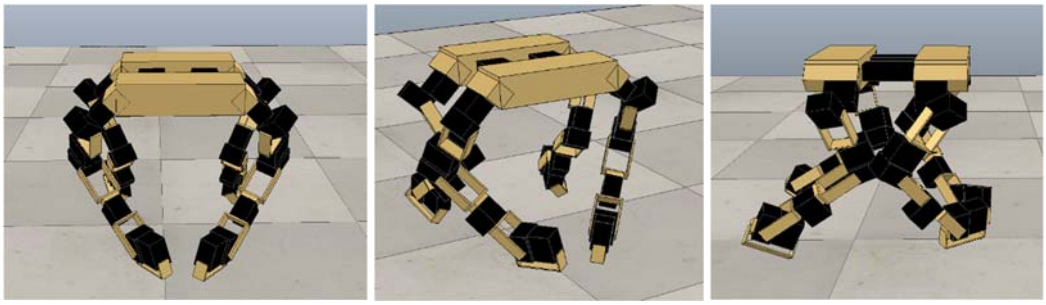

Figure 21. Images of the simulated robot in the fearful pose.

From Figure 14 and Figure 15, it can be seen that the happy pose has a lowered rear end, which indicates that there is no intention to run away and the front legs are spread open which shows intentional vulnerability and trust. The sad pose (Figure 16 and Figure 17) show a robot that has a lower front end and elbow angles visibly similar to neutral. Sadness is also much slower than neutral to make a display of a dejected shuffle. Anger (Figure 18 and Figure 19) has a level body and spread rear knees; the body is also slightly lower, and these give the image of a robot poised and ready to attack. Figure 20 and Figure 21 show the robot in a fearful pose. This is represented in both front and rear knees pointed inwards, as well as feet that are drawn in to the body to show a cowering motion.

One method of creating these poses is to lower the maximum torque setting of the physical robot, and to implement a control algorithm that makes the left side of the robot mirror the right side of the robot. With these settings, all four legs of the physical robot can be easily manipulated by a single researcher moving half of the robot by hand. This manipulation can continue until the pose matches a desired emotion and at that point, a snapshot of all the joint angles should be taken and stored. This method also ensures the necessary symmetry along the midsagittal plane. However, the lower torque settings may cause the robot to collapse under the force of gravity; in this case, the robot should be suspended by an external support, or a computed torque technique should be used to compensate for gravity.

Emotional Overlay

Finally, with the robot in a set of joint angles representing a pose, the CPG can then be run to create an emotive gait. This can be analogously viewed as perturbating the robot from neutral throughout the entire default gait. This perturbation creates keyframes, which initially match the emotive pose, and it is this perturbation that gives the gait its emotive qualities. These perturbations from neutral can be seen in Table 3 to Table 6.

As the CPG is running, the body maintains the same posture as created by the emotive pose. In addition to the body posture, the legs maintain their individual postures throughout their trajectories. This is facilitated by the redundant DOF, and is what allows the robot to maintain a dominating posture while angry or a cowering posture when fearful.

To further exaggerate these emotions, it is proposed that the CPG should be given a speed factor to increase or decrease the walking speed. This speed factor can also control the direction of motion. By controlling the direction of motion, the fearful robot can back away, as is instinctual when presented with something fearful.

It is important to note, however, that by making significant perturbations from neutral, modeling errors may become more evident. This can be seen in the happy pose of Figure 1; in this pose, any mass or link length errors will become more evident due to the front leg's extension in front of the robot's body and the corresponding increase in actuator torques

due to gravity. For this reason, it is necessary to individually tune the size of the CPG's buffered polygon for each emotion in order to maintain balance throughout all of the various gaits. In some cases, however, balancing the gait with a pose overlaid can cause dynamics from the body and leg motion that makes balancing impossible with the algorithm described. In these cases, the pose's deviations from neutral must be incrementally decreased until balancing is possible again. The possible need to bring an emotive pose back to neutral to maintain balance is one benefit to describing each pose relative to neutral. With this description, the increment may be defined by the normal of the pose's definition and this normalized vector may be subtracted from the pose until the emotive gait can be satisfactorily run without tipping.

3. EVALUATION SCHEMA

With emotive gaits now developed, an evaluation of their effectiveness must be done. The evaluation of this research includes both an external pilot study and an internal pilot study. The external pilot study is used to get feedback on the gaits with a specific effort of improving them. In this study, the subjects will be told what emotion the robot is trying to display, and the subjects will be asked for feedback on how to make the display more effective. The internal pilot study, however, only tries to measure the effectiveness of the gaits, and the subjects are not told beforehand what the emotive goal of the robot is. For both studies, IRB approval was obtained, under reference number IRB_00099688 with the IRB decision documentation shown in Appendix C.

External Pilot Study

The first study included five subjects who were tasked with verifying that the designed poses led to an elicitation of the desired emotions. In this study, the subject was shown the simulated robot walking with an overlaid emotion. After being told what the desired emotion was and having seen the

gait, the subject was asked to give qualitative suggestions to make the pose more effective at displaying the emotion being reviewed. The parameters about which the subjects were asked to give feedback included:

- The speed of the robot
- The maximum height of the foot bed throughout each step
- The step length of the swinging end effectors
- The initial position of the front and rear elbows (whether they should be closer or farther from the body)
- The initial position of the front and rear feet (whether they should be moved forward/backward or in/out)
- The height of the body throughout the demonstration of the gait
- The orientation of the body (whether it should be tilted more forward or backward)

The five subjects consisted of three males and two females with an average age of 29.4 years old. Because the subjects were told what the desired emotion was when it was displayed, potential subjects were not excluded from the study if they had prior knowledge of the research. Potential subjects were excluded, however, if they had impaired vision that prohibited them from viewing the simulation or if they had been diagnosed with a disorder that prevented them from recognizing intended emotions (such as autism). A blank study form can be seen in Figure 22.

This study led to poses that the subjects suggested were more effective

Emotion: _____

Improvements:

Speed: _____

Step Height: _____

Step Length: _____

Initial Elbow position (closer or farther from the body)
Front Elbow Position: _____
Rear Elbow Position: _____

Initial Feet Position (more forward/backward and/or more in or out)
Initial Front Feet Positions: _____
Initial Rear Feet Position: _____

Body Height: _____

Body Orientation (Tilted forward or backwards): _____
_____

Other Comments:_____
_____

Figure 22. A copy of the external pilot study form given to subjects.

at their intentional displays. After the data were gathered, the results were averaged and applied to each gait. In many cases, the suggested alterations made balancing impossible with the COP algorithm used, and the parameters had to be brought closer to neutral for the robot to successfully walk (as the creation of the emotional overlay describes).

Internal Pilot Study

After the feedback from the external study was implemented, an additional pilot study was executed to determine the overlaid gaits' effectiveness at conveying emotions. These tests used five new subjects, and in addition to the potential subject exclusions that applied to the external pilot study, these tests excluded anybody who had prior knowledge of the research. The five subjects chosen consisted of four males and one female, with an average age of 24.8 years old. To introduce the research, subjects were given an IRB approved cover letter that detailed the study's objectives and risks, which can be seen in Figure 23. If the subjects had no questions, they were then administered the tests.

The study was comprised of three blocks; in each block, the five gaits were displayed to the subject in a random order. After a gait was displayed, the subject was asked to mark which emotion they thought the robot was trying to emote. The subjects were told that they may mark the same emotion more than once throughout the block. A blank form can be seen in Figure 24.

Consent Cover Letter

Quadrupedal Emotive Gaits in Robotics

The purpose of this research study is to explore a robot's capability to display emotions utilizing its walking behavior (gait). In particular, the robot is going to try to show that it is: happy, sad, angry, afraid, and neutral. We are doing this study in an effort to improve human-robot interaction and bring mobile robots closer to having a common place in the home, this robotic behavior also has potential to be a strong tool in the field of therapeutic robotics.

The robot is going to walk towards you at a slow pace trying to exemplify one of its emotions five different times. Each time it walks towards you, you will be asked to mark what emotion you think it is trying to convey, and you may mark the same emotion more than once. This same test of gaits will be repeated two more times, though in a different order each round. Again, you will be asked to mark the emotion that you think the robot is trying to display after each gait. The robot will be tethered to the wall so that it cannot reach you and there is no foreseeable risk to you while completing this survey.

By completing this survey, you agree that you are over 18, have not been documented with a mental illness that will impair your ability to empathize and interpret emotions, you have unimpaired vision (corrective lenses will be allowed), and that you agree to allow your responses to be used for research purposes. The only personal information that will be recorded is your gender and your age, no identifying information will be marked or handled by researchers.

If you have any questions, complaints or if you feel you have been harmed by this research please contact Travis Hainsworth from the Department of Mechanical Engineering at the University of Utah at 801-913-2841.

Contact the Institutional Review Board (IRB) if you have questions regarding your rights as a research participant. Also, contact the IRB if you have questions, complaints or concerns which you do not feel you can discuss with the investigator. The University of Utah IRB may be reached by phone at (801) 581-3655 or by e-mail at irb@hsc.utah.edu.

It should take 15 to 30 minutes to complete this survey. Participation in this study is voluntary. You can choose not to take part. You can choose not to finish the questionnaire or omit any question you prefer not to answer without penalty or loss of benefits.

By returning this survey, you are giving your consent to participate.

Thank you very much for your time and willingness to participate in this study.

Sincerely,
Travis Hainsworth

FOOTER FOR IRB USE ONLY
Version: 112011

Figure 23. Cover letter provided to research subjects of the internal pilot study. The cover letter pilot studies were approved by the IRB.

.

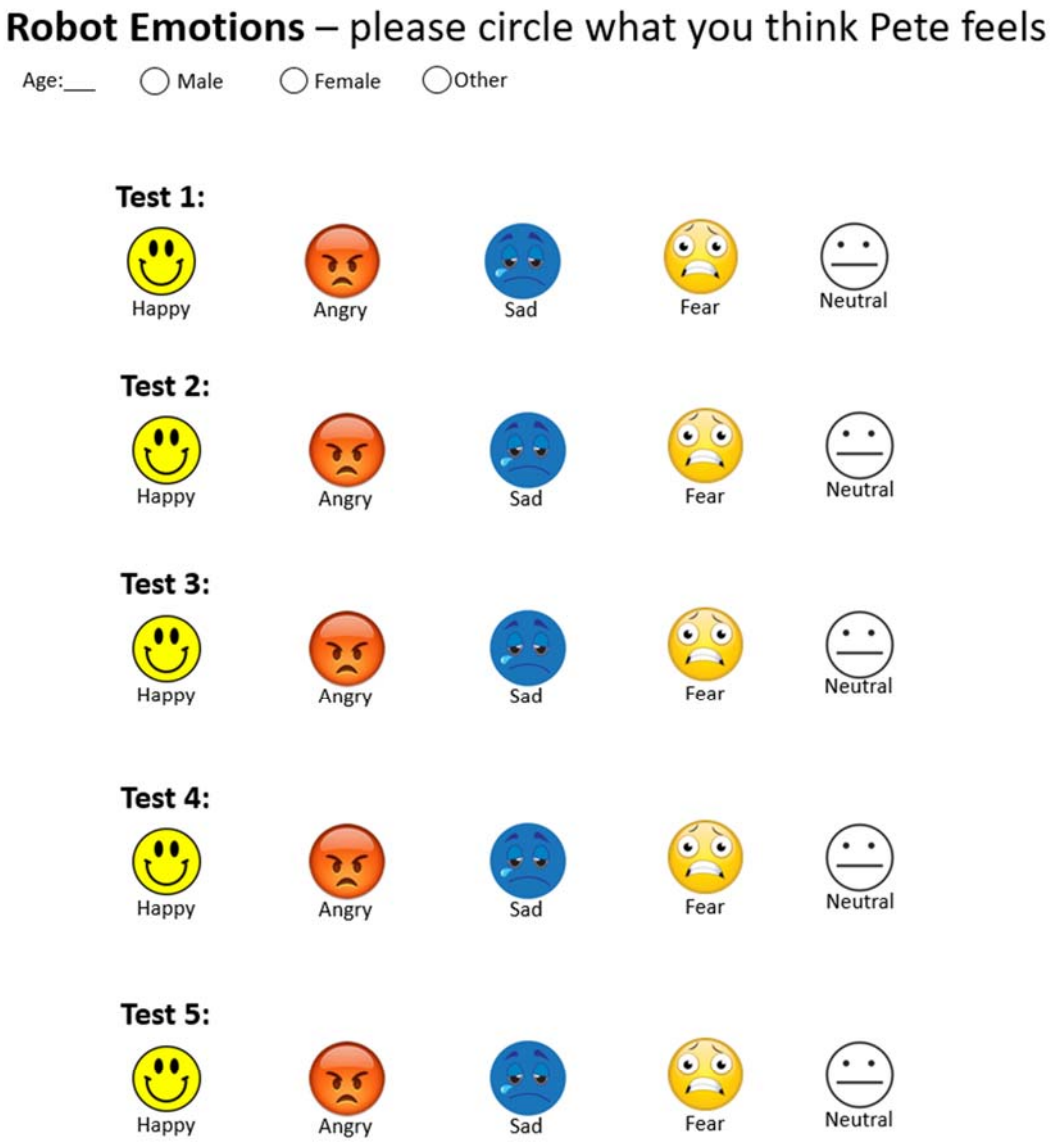

Figure 24. Copy of the internal pilot study's initial block of tests.

4. RESULTS

External Pilot Study Results

After administering the external pilot study to the five subjects, their feedback was averaged and implemented into the original emotive poses. In this study, the subjects were asked for qualitative suggestions, and this led to a need for qualitative averaging; the results of this averaged subject feedback can be seen in Table 7. The implementation of this feedback led to new

Table 7. Qualitative results from the external pilot study.

	Pose			
	Happy	**Sad**	**Angry**	**Scared**
Speed	Faster	Slower	Faster	Same
Step Height	Higher	Same	Much Higher	Lower
Step Length	Slightly Longer	Same	Increase	Same
Front Elbow Position	Same	Closer Together	Closer Together	Same
Rear Elbow Position	Same	Same	Same	Same
Initial Front Feet Positions	Move Feet Inwards	Slightly Farther Apart	Slightly Out	Same
Initial Rear Feet Positions	Same	Same	Same	Same
Body Height	Same	Same	Slightly Higher	Same
Body Orientation	Same	Same	Same	Tilt Forward

emotional overlays, and as the process of overlaying is described, some of the new poses were unstable and required decremental changes towards neutral. The final, stable poses can be seen in Figure 12 through Figure 21. The feedback and stabilization created significant changes for the original poses; the changes from these initial poses can be seen in Table 8 through Table 11.

As Ekman found, major emotions are cross cultural [7], but every individual has nuances when expressing these emotions. By taking feedback from multiple subjects and applying it to each pose, the nuances created by a single researcher's opinion on emotive displays were fleshed out, in turn creating a more universally identifiable display of robotic emotions.

Internal Pilot Study Results

With updated emotive poses now capable of being overlaid onto the CPG, it is necessary to evaluate each emotive gait's effectiveness. At this

Table 8. Changes from the initial happy pose to the final happy pose. These changes are based on subject feedback and stability requirements.

	Deviation from Initial Pose		
	X	Y	Z
Front Left Foot Position (mm)	-80	-60	-10
Front Left Foot Euler Angles (deg)	0	0	0
Front Left Foot Elbow Angle (deg)	25		
Front Step Height (mm)	0		
Hind Left Foot Position (mm)	15	-15	-10
Hind Left Foot Euler Angles (deg)	0	0	0
Hind Left Foot Elbow Angle (deg)	0		
Hind Step Height (mm)	0		
Step Length (mm)	-10		

Table 9. Changes from the initial angry pose to the final angry pose. These changes are based on subject feedback and stability requirements.

	Deviation from Initial Pose		
	X	Y	Z
Front Left Foot Position (mm)	-5	30	0
Front Left Foot Euler Angles (deg)	0	0	0
Front Left Foot Elbow Angle (deg)	40		
Front Step Height (mm)	20		
Hind Left Foot Position (mm)	-25	55	0
Hind Left Foot Euler Angles (deg)	0	0	0
Hind Left Foot Elbow Angle (deg)	-10		
Hind Step Height (mm)	20		
Step Length (mm)	20		

Table 10. Changes from the initial fearful pose to the final fearful pose. These changes are based on subject feedback and stability requirements.

	Deviation from Initial Pose		
	X	Y	Z
Front Left Foot Position (mm)	-30	0	-15
Front Left Foot Euler Angles (deg)	0	0	0
Front Left Foot Elbow Angle (deg)	0		
Front Step Height (mm)	-10		
Hind Left Foot Position (mm)	-30	0	-25
Hind Left Foot Euler Angles (deg)	0	0	0
Hind Left Foot Elbow Angle (deg)	0		
Hind Step Height (mm)	-10		
Step Length (mm)	0		

point, however, it became evident that the physical robot did not have the actuation torque required to display the gaits. This led to the simulation of the robot being used to complete the internal pilot study. The five new subjects gave results to the internal pilot study that can be seen in Table 12. These results show that four out of five emotions (including neutral) were

Table 11. Changes from the initial sad pose to the final sad pose. These changes are based on subject feedback and stability requirements.

	Deviation from Initial Pose		
	X	Y	Z
Front Left Foot Position (mm)	-25	0	-42.5
Front Left Foot Euler Angles (deg)	0	0	0
Front Left Foot Elbow Angle (deg)	10		
Front Step Height (mm)	10		
Hind Left Foot Position (mm)	15	0	0
Hind Left Foot Euler Angles (deg)	0	0	0
Hind Left Foot Elbow Angle (deg)	20		
Hind Step Height (mm)	55		
Step Length (mm)	0		

Table 12: A compilation of all of the results from the internal pilot study.

		Recognition Result (%)				
		Neutral	Happy	Sad	Anger	Fear
Emitted Emotion	Neutral	87	13			
	Happy	13	73	7		7
	Sad			33		67
	Anger	26		7	60	7
	Fear	7		33		60

successfully identified at least 60% of the time. Sadness was only identified 33% of the time, yet every misidentification of this gait was attributed to the fearful emotion.

Intuitively it seems that once a subject has been exposed to all of the gaits, their ability to successfully identify emotional poses should increase. To test this notion, each subject's final block of tests was compiled and can be seen in Table 13. The results of this summation show that three emotions are more successfully identified, one emotion's identification rate remains the

Table 13. The summation of results from the final block of tests of each subject in the internal pilot study.

		Recognition Result (%)				
		Neutral	Happy	Sad	Anger	Fear
Emitted Emotion	Neutral	80	20			
	Happy	20	80			
	Sad			60		40
	Anger	20			60	20
	Fear			20		80

same, yet the neutral gait was misidentified more often. After the subjects were exposed to all of the gaits, each emotion did, however, have a 60% identification rate or higher, including sadness.

5. ANALYSIS

Rejecting the Null Hypothesis

Due to the categorical nature of the data, the traditional chi-squared method can be implemented when analyzing the statistical independence of the different emotive gaits [36]. Categorical data can be tabularized, and the chi-squared statistical analysis utilizes tallies of each category's response. The actual chi-squared (χ^2) value of each table entry is computed with the equation:

$$\chi^2 = \sum \frac{(O_i - E_i)^2}{E_i}$$

where O_i is the observed table entry's tally and E_i is the expected tally. When conducting a test regarding the independence of variables, the chi-squared method compares the number of observed tallies with the number of expected tallies. When applying this to a null hypothesis test, the number of expected counts (E_i) would be an equal distribution.

In this research, the null hypothesis is: given a gait, there is equal probability that a subject will attribute it to any of the five provided emotions, or in other words, that the subject's perception of the robot's emitted emotion is independent of the gait that they are shown. The results

of the internal pilot study summarized in Table 12 give rise to the chi-squared independence table seen in Table 14**.** The summation of each table entry's χ^2 value leads to a total χ^2 of 135.29, but due to the low sample size, it is possible that this value is overestimated [36]. After comparing this value to a table of chi-squared distribution values (Table 1.3.6.7.4.1 in [37]), it can be seen that the null hypothesis can be easily rejected with a significance level of $\alpha = 0.05$. For this significance level of 0.05, χ^2 must be greater than 26.296, meaning we have a factor of safety of about 5; this factor of safety provides a comfortable buffer for the possible χ^2 overestimation.

Table 14. A chi-squared independence test from the results in Table 12. The top numbers are the number of observed values; the middle, italicized numbers are the number of expected values; and the bottom numbers in parentheses are the individual χ^2 values.

		Chi-Squared Independence Test				
		Neutral	Happy	Sad	Anger	Fear
Emitted Emotion	Neutral	13 *3* (33.33)	2 *3* (0.33)	0 *3* (3)	0 *3* (3)	0 *3* (3)
	Happy	2 *3* (0.33)	11 *3* (21.33)	1 *3* (1.33)	0 *3* (3)	1 *3* (1.33)
	Sad	0 *3* (3)	0 *3* (3)	5 *3* (1.33)	0 *3* (3)	10 *3* (16.33)
	Anger	4 *3* (0.33)	0 *3* (3)	1 *3* (1.33)	9 *3* (12)	1 *3* (1.33)
	Fear	1 *3* (1.33)	0 *3* (3)	5 *3* (1.33)	0 *3* (3)	9 *3* (12)

Qualitative Analysis

Though the chi-squared analysis proves that there is a correlation between a pose overlaid on a neutral gait and a user's interpretation of the robot's emotion, it does not explicitly state what that correlation is. From the internal pilot study's results in Table 12, it is evident that all poses except sad created identifiable gaits over 50% of the time and that sad was only mistaken for fear. Interestingly, previous studies demonstrated that subjects had difficulty distinguishing fear from other emotions as well [17]. Neutral was the most easily identifiable, and it was only mistaken for happy. Anger had the highest variance among all of the gaits, with the only emotion it wasn't mistaken for being happy. This seems to suggest that there are a wide array of perceptions concerning what an angry quadruped gait looks like.

Table 13 shows that after a subject has seen all of the overlaid gaits, they are more likely to identify the correct emotion, this suggests a large learning effect. Every emotion's correct perception rate increased from this learning effect, other than neutral's; neutral's identifiability was actually reduced by 7%. The largest increase in identifiability came from sadness, which increased by 27%. This learning effect suggests that a subject's perceptions adapt with repeated exposure to the gaits, which is key in the recognition and implementation of emotive gaits.

6. FUTURE WORK

As discussed, the analysis of Table 12 and the chi-squared independence test show that it is clearly possible for humans to interpret an intended display of emotions from a robotic quadruped's gait. However, it also suggests that the research in this area has yet to be finalized. There are a number of areas needing improvement that future work related to producing emotional displays in a quadruped's gait should examine. These improvements include enhancing the design of the robot, revising the CPG, and iterating upon the pose configurations.

The subject studies were limited by the fact that the surveys had to be conducted using the simulated robot instead of utilizing the real robot. This should be addressed by increasing the actuator torques. In addition to increasing actuator torques, the CPG could actively monitor torques and constantly prevent actuator saturation. Prevention of saturation could be done by decreasing the pose's deviations from neutral any time torque limits were exceeded, decreased to the point that the gait could physically proceed. After the actuators were no longer saturated, the pose deviations could then be increased back towards the original pose definitions. By improving the CPG in this manner, even if the physical robot were to remain unaltered, it

should still be able to run all the emotive poses through self-monitoring and automatic reconfigurations.

This need to correct configurations, however, is already done manually for balancing purposes, and is one contributing factor to the less than perfect internal study results. In order to maintain balance, the robot's emotional pose configurations had to be brought closer to neutral, in turn decreasing the poses emotive effect. Three things should be done to address this: the robot should be more accurately modeled, the full dynamics of the robot should be taken into consideration, and the balancing algorithm should be improved or changed to that of a dynamic gait. The inaccurate modeling of the robot prevents the system from remaining balanced when at the edge of the support polygon. This made the use of the buffered polygon required, and in turn created larger perturbations for balancing. Also, by not modeling the full dynamics of the robot, tipping often occurred at the point where the swing phase transitioned to a new foot. Finally, by limiting the balancing algorithm to only moving in the robot's y direction, larger than necessary movements had to be imposed; this further accentuated the previous two problems. If at this point the suggested poses still cannot be applied to the CPG without modifications, then a dynamic gait should be designed to take place of the crawl.

Despite over a 60% successful identification rate after the subjects had been exposed to the gaits and experienced the learning effect, the sad gait

still had only an overall successful identification rate of 30%, yet it was only ever mistaken as fear. This indicates that the poses are not wholly indicative of the emotions they attempt to portray and will need to be improved. For this reason, the external pilot study should be iterated upon, though the survey should be altered to be less open ended and more quantitative in an effort to produce more meaningful feedback. The next iteration of these tests should also be done on the real robot in an effort to remove any inconsistencies that may be created from subjects viewing the simulation.

After these improvements have been made, a larger study should be conducted in order to statistically ensure accurate results. For meaningful results with a medium effect size (which corresponds to a value of 0.3 based on Cohen's effect sizes [38]), a power of 0.8, and a significance level of 0.05; a pool of 15 subjects should be gathered and administered a study in the manner of the internal pilot study [39].

To expound on this work, a study could be done to test the effects of different magnitudes of emotions, such as an emphatic or subtle attempt at emitting a desired emotion. Describing the poses relative to neutral as presented here facilitates this test. As described, the poses could be decreased by a normalized amount for a subtler effect or increased in a similar manner for a more emphatic effect.

The gaits themselves could also be expounded upon. In this study, a method was presented to transform an existing gait into an emotive gait. It is

possible, however, to create a gait based solely on the display of a particular emotion. Perhaps a happy gait would dynamically bounce around, while an angry gait could oscillate between aggressive forward lurches and slow retreats, as if it were trying to intimidate an opponent into fleeing. Such notions could be explored by creating separate, unique gaits for each emotion (rather than overlaying an existing gait with all of the emotions).

Again, with a final success rate of 60% or higher for identification after learning, it seems evident that a robot can display emotions solely through its gait. However, these results also indicate that there is significant room for improvement. A few ways of improving include, but are not limited to: increasing the strength of the robot, improving the CPG to handle dynamics, improving the robustness of the balancing algorithm, and further tuning the poses through more subject studies. Developing these emotive gaits is just one step in the development of an empathetic robotic, but this research in combination with research regarding emotive actions and adding more emotive body parts (such as a head and tail) [2] could all culminate in a fully emotional robotic system.

7. CONCLUSION

This work clearly demonstrates that by varying a robot's pose as well as the speed, step height, and step length, a human can interpret a variety of emotions elicited by a robot. This research demonstrated this on a quadruped with 28 DOF, 7 of which comprise each leg. A closed form solution was found for the inverse kinematics of the legs that involved finding the inverse to Euler's finite rotation formula. This could be used, in pair with a CPG, to create a neutral crawl. Poses representing each emotion were then overlaid atop the neutral gait, and it is this overlaying of poses on top of neutral gaits that leads to movements that humans interpret as emotive.

The initial poses were iterated upon with an IRB approved study that was presented in Chapter 3. The feedback obtained from this initial study was implemented onto the robot and overlaid back onto the neutral gait. The final, iterated poses were then scrutinized by a new subject pool who evaluated each gaits' effectiveness with a second, different pilot study. The presented results of this study, shown in Table 7 and Table 12, support the hypothesis that a quadruped can walk in a manner that displays an intended emotion using the presented emotional poses in Figure 12 through Figure 21.

There is more work in this field of research to be done, but the

presented research provides a gateway to developing robotic systems designed for humans to emotionally bond with. Further work should include a more accurate model to be developed, along with stronger joint actuators to support the robot. In addition to physical changes, the CPG should be more robust in order to take consideration of the torque limits of the actuators into account. The poses should also be iterated upon with more subjects to make them more effective.

By developing robotic systems with intentional emotional displays robotics will become more viable solutions for therapeutic problems, they will be utilized as companion tools, and these systems will lead to more trust in medium-scaled robots, creating an easier gateway into the everyday home. Adapting walking to the display of emotions is one major step in the development of emotional robotics.

APPENDIX A

INVERSE OF EULER'S FINITE ROTATION FORMULA

Euler's Finite Rotation Formula

A vector $\boldsymbol{a}$ rotated by a fixed angle θ about a fixed unit vector $\boldsymbol{\eta}$ results in a new vector $\boldsymbol{b}$ with the following relationship:

$$\boldsymbol{b} = \boldsymbol{n} * (\boldsymbol{n} \cdot \boldsymbol{a}) * \big(1 - \cos(\theta)\big) + \boldsymbol{a} * \cos(\theta) + \boldsymbol{n} \times \boldsymbol{a} * \sin(\theta)$$

This finite rotation formula was first introduced by Leonhard Euler, but is commonly attributed to Olinde Rodrigues [26]. In this work, the inverse of this equation (obtaining θ given vectors $\boldsymbol{b}$, $\boldsymbol{a}$, and $\boldsymbol{n}$) is used to find the angle of the elbow when creating poses for the quadruped, and is also used in the inverse kinematics of the 7 DOF arm presented above.

Inverse of Euler's Finite Rotation Formula

The inverse of the finite rotation formula to find θ given the vectors $\boldsymbol{b}$, $\boldsymbol{a}$, and $\boldsymbol{n}$ can be found with an application of intelligent dot products. By taking the dot product of both sides of the finite rotation formula with $\boldsymbol{a}$, the cosine of θ can be isolated:

$$\cos(\theta) = \frac{\boldsymbol{a} \cdot \boldsymbol{b} - \boldsymbol{a} \cdot \boldsymbol{n} * (\boldsymbol{n} \cdot \boldsymbol{a})}{\boldsymbol{a} \cdot \boldsymbol{a} - \boldsymbol{a} \cdot \boldsymbol{n} * (\boldsymbol{n} \cdot \boldsymbol{a})}$$

Similarly, the sine of θ can be isolated by applying the dot product of $\boldsymbol{n} \times \boldsymbol{a}$ to the finite rotation formula:

$$\sin(\theta) = (\boldsymbol{n} \times \boldsymbol{a}) \cdot (\boldsymbol{b} - \boldsymbol{n} * (\boldsymbol{n} \cdot \boldsymbol{a}))$$

Then using the four-quadrant arctangent function, θ can be found:

$$\theta = \operatorname{atan2}(\sin(\theta), \cos(\theta))$$

APPENDIX B

INVERSE KINEMATICS CODE

The robot was programmed in C++ and the code for the inverse kinematics has been included here:

```
VectorXd Kinematics::GetJointAngles(Vector3d* Position, Matrix3d* Rotation, double
ThetaElbow, bool SingleLeg, bool TrackOldAngles) {
	VectorXd JointAngles(7);

	// Get rid of the base and tool frame
	if (SingleLeg == false)
		Convert_To_Leg(Position, Rotation);

	// Ensure that the desired location is not outside of the workspace
	if (Position->norm()*1.001 > d3 + d5) {
		//std::cout << "Desired location is out of reach." <<
(*Position).transpose() << "\n";
		Vector3d NewPos = *Position;
		while (NewPos.norm()*1.005 > d3 + d5)
			NewPos -= (NewPos / NewPos.norm()); // addition is a gain of
sorts

		try { JointAngles = GetJointAngles(&NewPos, Rotation, ThetaElbow,
true, true); }
		catch (const std::bad_alloc& e){
			std::cout << "Yo Shit Overflowed\n";
			return (*dhp).col(3);
		}
		return JointAngles;
	}

	// Solve for t4
	double t4 = 2 * atan(sqrt((pow(d3 + d5, 2) - pow((*Position).norm(), 2)) /
(pow((*Position).norm(), 2) - pow(d3 - d5, 2)))); // Elbow in vs Elbow Out
	t4 *= t4_force; // Forcing elbow in vs elbow out;

	// Solve for t1' and t2' using planar solution
	double t1p = atan2((*Position)(1), (*Position)(0)); // used to be atan

	Matrix3d A1p;
	A1p << cos(t1p), 0, sin(t1p),
		sin(t1p), 0, -cos(t1p),
		0, 1, 0;

	Vector3d p1wp = A1p.transpose()*(*Position);

	double phi = atan2(p1wp(1), p1wp(0));
	double psi = atan2(d5*sin(t4), d3 + d5*cos(t4));
	double t2p = phi - psi + M_PI / 2;

	// Solve t1 and t2
	Vector3d pep(d3*cos(t1p)*sin(t2p), d3*sin(t1p)*sin(t2p), -cos(t2p)*d3);

	Vector3d n = (*Position) / (*Position).norm();
	Vector3d pe = n*n.dot(pep)*(1 - cos(ThetaElbow)) + pep*cos(ThetaElbow) +
n.cross(pep)*sin(ThetaElbow);

	double t1 = atan2(pe(1), pe(0));
```

```
double t2_var = sqrt(pow(pe(0), 2) + pow(pe(1), 2));
if (t1_force == -1) {
	t1 += M_PI;
	t2_var = -t2_var;
}
double t2 = atan2(t2_var, -pe(2));
/////// Shoulder Degeneracy /////////
if (round(t2 * 100) == 0 || round(t2 * 100) == round(M_PI * 100)){
	t1 = 0;
	std::cout << "Singularity in shoulder entered \n";
}
//////////////////////////////////////

// Solve t3
Matrix4d Transf1; CreateT(0, 0, t1, M_PI / 2,Transf1);
Matrix4d Transf2; CreateT(0, 0, t2, M_PI / 2,Transf2);
Matrix4d Transf3; CreateT(0, d3, 0, -M_PI / 2,Transf3);
Matrix4d Transf4; CreateT(0, 0, t4, M_PI / 2,Transf4);
Matrix4d Transf5; CreateT(0, d5, 0, -M_PI / 2,Transf5);

Matrix4d Transf15 = Transf1*Transf2*Transf3*Transf4*Transf5;
Vector3d pw3p(Transf15(0, 3), Transf15(1, 3), Transf15(2, 3));
pw3p -= pe;

Vector3d Temp = *Position - pe;
double t3 = InverseRodrigues(&pw3p, &pe, &Temp);

////////// Knee Degeneracy ///////////
if (round(t4 * 100) == 0 || round(t4 * 100) == round(M_PI * 100)) {
	t3 = 0;
	std::cout << "Singularity in knee entered \n";
}
//////////////////////////////////////

// Find wrist position and solve for theta wrists
Matrix4d T3; CreateT(0, d3, t3, -M_PI / 2,T3);
Matrix4d T14 = Transf1*Transf2*T3*Transf4;
Matrix3d W4;
for (int row = 0; row < 3; row++) {
	for (int col = 0; col < 3; col++) {
		W4(row, col) = T14(row, col);
	}
}
Matrix3d W47 = W4.transpose()*(*Rotation);

double t5 = atan2(W47(1, 2), W47(0, 2));
if (flip_foot == true) t5 += M_PI;
while (t5 > M_PI) t5 -= 2 * M_PI;
while (t5 < -M_PI) t5 += 2 * M_PI;

double st6 = W47(0, 2)*cos(t5) + W47(1, 2)*sin(t5);
double ct6 = W47(2, 2);
double t6 = atan2(st6, ct6);


double st7 = -W47(0, 0)*sin(t5) + W47(1, 0)*cos(t5);
double ct7 = -W47(0, 1)*sin(t5) + W47(1, 1)*cos(t5);
```

```
	double t7 = atan2(st7, ct7);

	//////// Wrist Degeneracy ///////////
	if (abs(t6) < 0.001) {
		t7 = 0;
		t5 = atan2(W47(1, 0), W47(0, 0));
		std::cout << "Singularity in ankle entered \n";
	}
	if (round(t6 * 100) == round(M_PI * 100)) {
		t7 = 0;
		t5 = atan2(-W47(1, 0), -W47(0, 0));
		std::cout << "Singularity in ankle entered \n";
	}
	////////////////////////////////////


	JointAngles << t1, t2, t3, t4, t5, t6, t7;
	for (int i = 0; i < 7; i++) {
		while (JointAngles(i) > M_PI)
			JointAngles(i) -= 2 * M_PI;
		while (JointAngles(i) < -M_PI)
			JointAngles(i) += 2 * M_PI;
	}


	//////// Keep consitency of the p of Elbow and p of Foot ///////////
	// Obtain old Elbow position
	Matrix4d Telbow = Matrix4d::Identity();
	Matrix4d T_Current;
	for (int i = 0; i < 4; i++) {
		CreateT((*dhp)(i, 0), (*dhp)(i, 2), (*dhp)(i, 3), (*dhp)(i, 1),
T_Current);
		Telbow *= T_Current; // Using the old stored values
	}

	Elbow_Old << Telbow(0, 3), Telbow(1, 3), Telbow(2, 3);


	if (Old_Pos_Def == false) {
		Position_Old << (*Position)(0), (*Position)(1), (*Position)(2);
		Old_Pos_Def = true;
	}

	Vector3d OldCross = Elbow_Old.cross(Position_Old);
	Vector3d NewCross = pe.cross((*Position));

	if (OldCross.dot(NewCross)<0 && TrackOldAngles == true){// elbow in vs out
		if (ThetaElbow > 2 * M_PI) // Then this shit has gone on for to long
			t1_force *= -1;
		ThetaElbow += M_PI;
		JointAngles = GetJointAngles(Position, Rotation, ThetaElbow, true,
TrackOldAngles);
	}

	T_dot_old = this->T_dot;
	T_dot = JointAngles - (*dhp).col(3); // Store the change in angles for
Newton Euler
	(*dhp).col(3) = JointAngles; // Update the kinematics joint angles because
```

```
it does not seem to work else where
        Position_Old << (*Position)(0), (*Position)(1), (*Position)(2);
        Elbow_Old = pe;
        return JointAngles;
}
```

APPENDIX C

IRB APPROVAL DOCUMENTATION

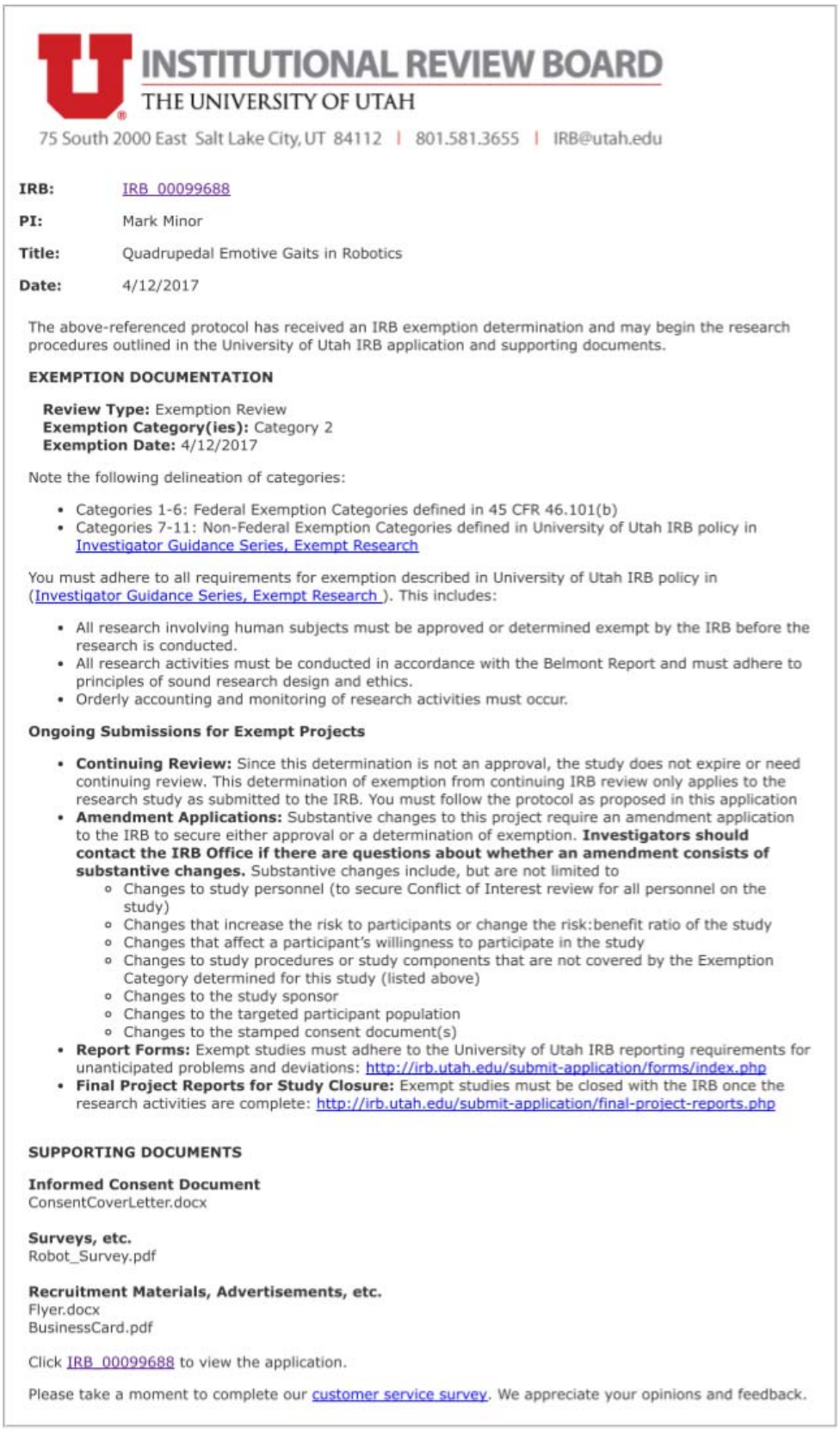

INSTITUTIONAL REVIEW BOARD
THE UNIVERSITY OF UTAH
75 South 2000 East Salt Lake City, UT 84112 | 801.581.3655 | IRB@utah.edu

IRB: IRB_00099688

PI: Mark Minor

Title: Quadrupedal Emotive Gaits in Robotics

Date: 4/12/2017

The above-referenced protocol has received an IRB exemption determination and may begin the research procedures outlined in the University of Utah IRB application and supporting documents.

EXEMPTION DOCUMENTATION

Review Type: Exemption Review
Exemption Category(ies): Category 2
Exemption Date: 4/12/2017

Note the following delineation of categories:

- Categories 1-6: Federal Exemption Categories defined in 45 CFR 46.101(b)
- Categories 7-11: Non-Federal Exemption Categories defined in University of Utah IRB policy in Investigator Guidance Series, Exempt Research

You must adhere to all requirements for exemption described in University of Utah IRB policy in (Investigator Guidance Series, Exempt Research). This includes:

- All research involving human subjects must be approved or determined exempt by the IRB before the research is conducted.
- All research activities must be conducted in accordance with the Belmont Report and must adhere to principles of sound research design and ethics.
- Orderly accounting and monitoring of research activities must occur.

Ongoing Submissions for Exempt Projects

- **Continuing Review:** Since this determination is not an approval, the study does not expire or need continuing review. This determination of exemption from continuing IRB review only applies to the research study as submitted to the IRB. You must follow the protocol as proposed in this application
- **Amendment Applications:** Substantive changes to this project require an amendment application to the IRB to secure either approval or a determination of exemption. **Investigators should contact the IRB Office if there are questions about whether an amendment consists of substantive changes.** Substantive changes include, but are not limited to
  - Changes to study personnel (to secure Conflict of Interest review for all personnel on the study)
  - Changes that increase the risk to participants or change the risk:benefit ratio of the study
  - Changes that affect a participant's willingness to participate in the study
  - Changes to study procedures or study components that are not covered by the Exemption Category determined for this study (listed above)
  - Changes to the study sponsor
  - Changes to the targeted participant population
  - Changes to the stamped consent document(s)
- **Report Forms:** Exempt studies must adhere to the University of Utah IRB reporting requirements for unanticipated problems and deviations: http://irb.utah.edu/submit-application/forms/index.php
- **Final Project Reports for Study Closure:** Exempt studies must be closed with the IRB once the research activities are complete: http://irb.utah.edu/submit-application/final-project-reports.php

SUPPORTING DOCUMENTS

Informed Consent Document
ConsentCoverLetter.docx

Surveys, etc.
Robot_Survey.pdf

Recruitment Materials, Advertisements, etc.
Flyer.docx
BusinessCard.pdf

Click IRB_00099688 to view the application.

Please take a moment to complete our customer service survey. We appreciate your opinions and feedback.

Figure 25. IRB approval documentation

REFERENCES

[1] B. Robins et al, "Robotic assistants in therapy and education of children with autism: can a small humanoid robot help encourage social interaction skills?," *Universal Access in the Information Society,* 2005, pp. 105-120.

[2] L. Moshkina and R. C. Arkin, "Human perspective on affective robotic behavior: A longitudinal study," in *Intelligent Robots and Systems, 2005.(IROS)*, 2005, pp. 1444-1451.

[3] M. Destephe et al, "Improving the human-robot interaction through emotive movements: a special case: walking," in *Proc. of the 8th ACM/IEEE Int. Conf. on Human-Robot Interaction*, 2013, pp. 115-116.

[4] C. L. Roether et al, "Critical features for the perception of emotion from gait," *Journal of Vision,* vol. 9, no. 6, pp. 15-47, Jun 26 2009.

[5] L. Zhao and N. I. Badler, "Synthesis and acquisition of laban movement analysis qualitative parameters for communicative gestures," Dept. of Comp. Sci., Univ. Pennsylvania, Philadelphia, PA, 2001.

[6] M. Lhommet et al, "Expressing Emotion Through Posture and Gesture," in *The Oxford Handbook of Affective Computing*, Oxford, UK, Oxford Univ. Press, 2014, pp. 1-21.

[7] P. Ekman and W. V. Friesen, "Constants across cultures in the face and emotion," *Journal of Personality and Social Psychology,* vol. 17, no. 2, 1971, pp. 124-129.

[8] C. Darwin, P. Ekman, and P. Prodger, *The expression of the emotions in man and animals*. Oxford, UK, Oxford Univ. Press, 1998.

[9] P. Ekman and H. Oster, "Facial expressions of emotion," *Annual Review of Psychology,* vol. 30, no. 1, pp. 527-554, 1979.

[10] P. Pongracz, C. Molnar, A. Miklosi, and V. Csanyi, "Human listeners are able to classify dog (Canis familiaris) barks recorded in different

situations," *Journal of Computational Psychology,* vol. 119, no. 2, pp. 136-44, May 2005.

[11] A. Barliya, L. Omlor, M. A. Giese, A. Berthoz, and T. Flash, "Expression of emotion in the kinematics of locomotion," *Experimental Brain Research,* vol. 225, no. 2, pp. 159-76, Mar 2013.

[12] T. Bloom and H. Friedman, "Classifying dogs' (Canis familiaris) facial expressions from photographs," *Behavioural Processes,* vol. 96, pp. 1-10, Jun 2013.

[13] N. Bolwig, "Facial expression in primates with remarks on a parallel development in certain carnivores (a preliminary report on work in progress)," *Behaviour,* vol. 22, no. 3, pp. 167-192, 1964.

[14] J. J. Collins and I. N. Stewart, "Coupled nonlinear oscillators and the symmetries of animal gaits," *Journal of Nonlinear Science,* vol. 3, no. 1, pp. 349-392, 1993.

[15] D. M. Nunamaker and P. D. Blauner, "Normal and abnormal gait," in *Textbook of small animal orthopaedics,* Philadelphia, PA, Lippincott Williams & Wilkins, 1985, ch. 91, pp. 1083-1095.

[16] T. Hashimoto, S. Hitramatsu, T. Tsuji, and H. Kobayashi, "Development of the face robot SAYA for rich facial expressions," in *SICE-ICASE, 2006. Int. Joint Conf.*, 2006, pp. 5423-5428.

[17] K. Berns and J. Hirth, "Control of facial expressions of the humanoid robot head ROMAN," in *Intelligent Robots and Systems, 2006 IEEE/RSJ Int. Conf.*, 2006, pp. 3119-3124.

[18] K. Amaya, A. Bruderlin, and T. Calvert, "Emotion from motion," in *Graphics Interface*, 1996, vol. 96, pp. 222-229.

[19] M. Karg, M. Schwimmbeck, K. Kühnlenz, and M. Buss, "Towards mapping emotive gait patterns from human to robot," in *RO-MAN, IEEE*, 2010, pp. 258-263.

[20] R. B. McGhee and A. A. Frank, "On the stability properties of quadruped creeping gaits," *Mathematical Biosciences,* vol. 3, pp. 331-351, 1968.

[21] M. Kalakrishnan et al, "Fast, robust quadruped locomotion over challenging terrain," in *Robotics and Automation (ICRA),* 2010, pp.

2665-2670.

[22] K. Byl et al, "Reliable dynamic motions for a stiff quadruped," in *Experimental Robotics*, Berlin, 2009, pp. 319-328.

[23] M. B. Colton et al, "Toward therapist-in-the-loop assistive robotics for children with autism and specific language impairment," in *AISB new frontiers in human-robot interaction symposium*, 2009, vol. 24, p. 25-30.

[24] B. Siciliano, "Kinematic control of redundant robot manipulators: A tutorial," *Journal of Intelligent & Robotic Systems,* vol. 3, no. 3, pp. 201-212, 1990.

[25] J. M. Hollerbach, "Optimum kinematic design for a seven degree of freedom manipulator," in *Robotics research: The second international symposium*, 1985, pp. 215-222.

[26] K. Gupta, "An historical note on finite rotations," *Journal of Applied Mechanics,* vol. 56, p. 139, 1989.

[27] J. M. Hollerbach, "Chapter 5: Inverse Kinematics for Position," unpublished.

[28] H. Hwang and Y. Youm, "Dynamic crawl gait algorithm for quadruped robots," in *Intelligent Robots and Systems*, 2008, pp. 1507-1512.

[29] D.-O. Kang et al, "A study on an adaptive gait for a quadruped walking robot under external forces," in *Robotics and Automation*, 1997, vol. 4, pp. 2777-2782.

[30] F. Hardarson, "Stability analysis and synthesis of statically balanced walking for quadruped robots," Ph.D. dissertation, Dept. Mach. Design, Royal Inst. of Tech., Stockholm, Sweden, 2002.

[31] M. VukobratoviĆ and B. Borovac, "Zero-Moment Point — Thirty Five Years of Its Life," *International Journal of Humanoid Robotics,* vol. 01, no. 01, pp. 157-173, 2004.

[32] Sky. (2012, 5/27/2017). *Reading Dog Body Language*. Available: https://blogslobbertraining.wordpress.com/tag/happy/

[33] S. Delaney. (2016, 5/27/2017). *Child's Best Friend: Dog Bite Prevention*. Available: http://www.wisconsinfederatedhs.org/medical-

tips1

[34] A. Rift. (2009, 5/27/2017). *Very Angry Dog*. Available: https://www.youtube.com/watch?v=rmO8jy7sHeY

[35] DOL. (2014, 5/27/2017). *Fearful/Shy Dog Workshop*. Available: http://www.dogsoutloud.org/fearful-shy-dog-workshop/#/

[36] R. J. Light, "Measures of response agreement for qualitative data: Some generalizations and alternatives," *Psychological Bulletin,* vol. 76, no. 5, p. 365, 1971.

[37] NIST/SEMATECH, e-Handbook of Statistical Methods, 2003. [Online]. Available: http://www.itl.nist.gov/div898/handbook/. Accessed on 5/22/2017.

[38] J. Cohen, "Statistical power analysis for the behavioral sciences," *Hillsdale, NJ,* pp. 20-26, 1988.

[39] Q. Bioinformatics. (2015, 5/22/2017). *ANZMTG Statistical Decision Tree, Power Calculator (1 ed.)*. Available: http://www.anzmtg.org/stats/PowerCalculator